General Disclaimer

One or more of the Following Statements may affect this Document

- This document has been reproduced from the best copy furnished by the organizational source. It is being released in the interest of making available as much information as possible.

- This document may contain data, which exceeds the sheet parameters. It was furnished in this condition by the organizational source and is the best copy available.

- This document may contain tone-on-tone or color graphs, charts and/or pictures, which have been reproduced in black and white.

- This document is paginated as submitted by the original source.

- Portions of this document are not fully legible due to the historical nature of some of the material. However, it is the best reproduction available from the original submission.
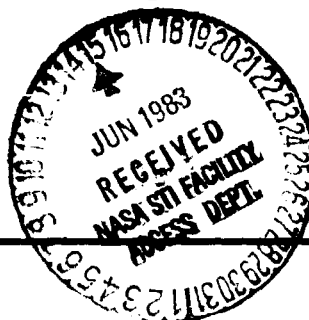
NASA

Technical Memorandum 83985

The Sensitivity of Numerically Simulated Climates to Land-Surface Boundary Conditions

Yale Mintz

August 1982

Laboratory for Atmospheric Sciences
Modeling and Simulation Facility

Now in press, as a
chapter in _The Global Climate_,
edited by J. T. Houghton.
Cambridge University Press,
Cambr./London/N.Y. (Scheduled
for publication in summer 1983.)

THE SENSITIVITY OF NUMERICALLY SIMULATED CLIMATES

TO LAND-SURFACE BOUNDARY CONDITIONS*

by

Yale Mintz

Department of Meteorology
University of Maryland, College Park, MD 20742

and

Laboratory for Atmospheric Sciences
NASA Goddard Space Flight Center, Greenbelt, MD 20771

ABSTRACT

This review describes, interprets, and compares eleven sensitivity experiments that have been made with general circulation models to see how land-surface boundary conditions can influence the rainfall, temperature, and motion fields of the atmosphere. In one group of experiments, different soil moistures or albedos are prescribed as time-invariant boundary conditions. In a second group, different soil moistures or different albedos are initially prescribed, and the soil moisture (but not the albedo) is allowed to change with time according to the governing equations for soil moisture. In a third group, the results of constant versus time-dependent soil moistures are compared.

All of the experiments show that the atmosphere is sensitive to the land-surface evapotranspiration: so that changes in the available soil moisture or changes in the albedo (which affects the energy available for evapotranspiration) produce large changes in the numerically simulated climates.

TABLE OF CONTENTS

Some Observational and Theoretical Considerations.

Averaged for the globe and for the year, the measured river water drainage from the continents is about a third as large as the measured precipitation (Baumgartner and Reichel, 1975, Table 9; Korzun, 1978, Table 150). This means that on the average the land-surface evapotranspiration is about two-thirds as large as the precipitation.

In some continental regions, during part of the year, the evapotranspiration is larger than the precipitation. This cannot be known from measurements of river flow, but can be derived from measurements of the transport of water vapor by the atmosphere. An example of this for the central and eastern United States, in July, is shown in Fig. 1.

On the left in the figure is the vertical distribution of the water vapor transport divergence, as given by twice daily rawinsonde measurements for two July months, and averaged for the region 80°W-100°W, 30°N-47.5°N, which is an area of about $(2000 \text{ km})^2$ (Rasmusson, 1968, Table 1 and Fig. 2). From the surface to the 930 mb level there is a water vapor transport convergence of 1.4 gm cm^{-2} month^{-1}: or 14 mm/mo equivalent water depth. Above the 930 mb level there is divergence of 36 mm/mo. Integrated over the entire depth of the atmosphere there is a net divergence (a net removal of water from the region) of 22 mm/mo.

From the beginning to the end of July the change in the water vapor content of the atmosphere is very small. Therefore, the 22 mm of water that are removed from the region must come from the water stored in the soil; which means that the evapotranspiration is 22 mm/mo larger than the precipitation. Inasmuch as the measured average July precipitation in this region is about
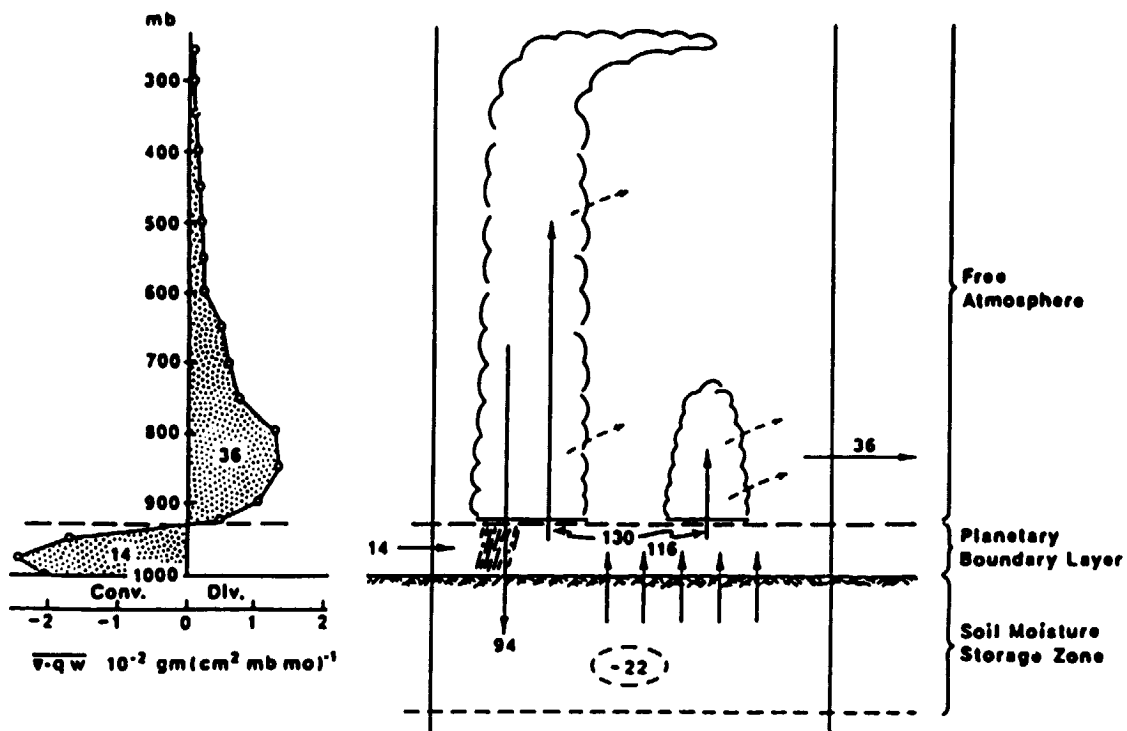
Fig. 1   Water budget (mm/mo) for the central and eastern United States, in July. Divergence of the water vapor transport is from Rasmusson (1968).

94 mm/mo, the average July evapotranspiration must be about 116 mm/mo (3.7 mm/day). [A comparable analysis for the central and eastern United States by Benton et al. (1953, Figs. 24, 26) gave a July evapotranspiration of 121 mm/mo (3.9 mm/day)]. We can interpret this water budget as follows:

The July net radiational heating of the ground in this region, in July, is about 140 watt/m^2 (Budyko, 1963, Plate 21), which if used entirely for evapotranspiration would put about 150 mm/mo (4.8 mm/day) of water into the air. But if we accept the aerologically derived evapotranspiration of 3.7 mm/day (LE = 107 watt/m^2), there will be a sensible heat transfer from the ground to the atmosphere, H = (R_N - LE) = (140 - 107) = 33 watt/m^2; and a Bowen ratio, (H/LE), equal to 0.31.

The 116 mm/mo of water vapor, forced into the atmospheric planetary boundary layer by the radiational heating of the surface, combines with the 14 mm/mo brought into the region by the water vapor transport convergence in the boundary layer; and the total of 130 mm/mo of water vapor are transferred from the boundary layer to the free atmosphere.

In July, the condensation and precipitation in this region is predominantly of the convective type, with relatively little large-scale upglide condensation and precipitation. Therefore, the transfer of water vapor upward from the surface is predominantly by small scale turbulent mixing within the planetary boundary layer, with a handover to cumulus convection which carries the water vapor from the top of the boundary layer into the free atmosphere.

Of the 130 mm/mo of moisture carried into the free atmosphere by the cumulus cloud towers, 36 mm/mo (in the form of water vapor, liquid water droplets and ice crystals) are detrained from the clouds into the cloud

environment (where the water droplets and ice crystals evaporate) and are removed from the region by the divergence of the water vapor transport in the free atmosphere. The remaining 94 mm/mo return to the earth's surface as the convective precipitation. The excess of the evapotranspiration over the precipitation, 22 mm/mo, is the moisture withdrawn from the soil.

According to this analysis, the convective precipitation draws all of its moisture from the water vapor in the planetary boundary layer; and the amount of water vapor supplied to the boundary layer by the surface evapotranspiration is an order of magnitude larger than the amount supplied by the water vapor transport convergence. This suggests that the surface evapotranspiration is the main determinant of the precipitation.

[The winter season water budget over the central and eastern United States is very different from that shown in Fig. 1. In winter the water vapor transport convergence does not change sign with height, but is convergent at all levels and produces a net import of water vapor to the region (Rasmusson, 1968, Table 1 and Fig. 2). In winter, the condensation and precipitation is predominantly of the large-scale upglide condensation type (frontal cloud and precipitation) which draws from the water vapor at all levels in the troposphere. Moreover, in winter the net radiational heating of the ground is small (Budyko, 1963, plate 15) and, consequently, over the unforested part of this region the evapotranspiration is small. In winter, therefore, the land-surface evapotranspiration cannot have much influence on the precipitation or other fields. It is only in the tropics and in the summer season extratropics, where evapotranspiration is large and where the precipitation is of the type that draws its water vapor from the planetary boundary layer, that the land-surface evapotranspiration can be of major importance.]

With respect to the tropics and the summer season extratropics, two questions immediately come to mind:

1)   If the surface evapotranspiration, by some means, is greatly reduced, can the boundary layer water vapor transport convergence increase by a corresponding amount and, in that way, maintain the precipitation? And,

ii)   If the surface evapotranspiration and the boundary layer water vapor transport convergence remain the same, can an increased detrainment and water vapor transport divergence in the free atmosphere stop the precipitation?

● To answer the first question, we write the water vapor transport convergence as $-\nabla \cdot q\, \mathbf{v} = -\mathbf{v} \cdot \nabla q - q \nabla \cdot \mathbf{v}$, where q is the water vapor mixing ratio and $\mathbf{v}$ is the horizontal velocity of the air.

$-\mathbf{v} \cdot \nabla q$ is positive when the air that leaves the region is drier than the air that enters. But if this drying is due to the removal of water vapor from the boundary layer by cumulus convection, then the convection will stop as soon as there is a small reduction in the boundary layer water vapor content. $-\mathbf{v} \cdot \nabla q$ cannot maintain the observed rate of precipitation over a distance which is greater than just a few cumulus convection cells; say, a total distance of a few kilometers.

The other term, $-q \nabla \cdot \mathbf{v}$, also can maintain the observed rate of precipitation only over a restricted domain in the extratropics. The water vapor mixing ratio, in the boundary layer of a maritime tropical air mass over the extratropical continents in summer, is of the order of 10 parts per thousand. Therefore, a boundary layer that is 100 mb (1 km) deep must have a horizontal velocity convergence, $-\nabla \cdot \mathbf{v}$, of 0.37 day^{-1} (0.43 x 10^{-5} sec^{-1}) to produce a water vapor transport convergence of 3.7 mm/day. The characteristic velocity of the boundary layer air in the extratropics, in summer, is 2 to 3 m/s; and the angle between this vector velocity and the streamline of the

non-divergent flow, integrated over the depth $_\wedge^{of}$ the boundary layer, is about 10°.
Thus, if we consider the circular region with radius r, we have $-\nabla \cdot \mathbf{v} =$
0.43×10^{-5} s^{-1} = (3 m s^{-1} sin 10°) $2\pi r/\pi r^2$; or r = 240 km, and 480 km is
the limiting diameter of the region where water vapor transport convergence
in the boundary layer can produce the observed rate of precipitation.

In the extratropics, therefore, there is a size limit, of the order
of a few hundred kilometers, beyond which   boundary layer water vapor
transport convergence cannot compensate for diminished evapotranspiration.
It is only near the equator, where the divergent component of the velocity
field is larger and the planetary boundary layer is deeper, that there can
be appreciable water vapor transport convergence over a much larger sized
area.

●● The answer to the second question, "Can an increased detrainment and
water vapor transport divergence in the free atmosphere stop the precipita-
tion?", depends on whether the free atmosphere is supplied with dry air into
which the cumulus cloud towers can detrain. That will happen only if, in
addition to the boundary layer mass (and water vapor) convergence, there is
also a mass convergence in the uppermost troposphere. Then, the cumulus
cloud towers can detrain all of the water into the subsiding and diverging
dry air of the middle troposphere, and not produce any precipitation at all.
The best known example of extensive fields of non-precipitating cumulus
clouds of this kind are the Trade Wind cumuli over the tropical oceans,
where the subsiding air in the middle troposphere has its origin in the high
level outflow above the intertropical convergence zone. We also see such
fair weather cumulus clouds removing   water vapor from the boundary
layer, without producing precipitation, west of the trough lines and east
of the ridge lines of the fast-transient and slow-transient waves in the

extratropical westerlies, where both the longitudinal and the latitudinal scale can be as large as a few thousand kilometers. We can say, therefore, that on a scale larger than a few hundred kilometers, in the extratropics, land-surface evapotranspiration is a necessary (but not sufficient) condition for convective precipitation. The upper tropospheric circulation must also be favorable for precipitation.

Because so many interactive thermodynamical and hydrodynamical processes are involved, the best way to determine the overall influence of the land-surface boundary conditions on the rainfall, temperature and circulation is through experiments with atmospheric general circulation models. Existing general circulation models have been fairly successful in simulating the observed climate of the earth, including the principle geographical and seasonal characteristics of the precipitation (WMO, 1979). By making pairs of time-integrations, with all of the initial conditions and boundary conditions the same except for those which can affect the land-surface evapotranspiration, and comparing the two solutions, we can ascertain what the land-surface influence is.

In the existing general circulation models, the two boundary conditions that can affect the land-surface evapotranspiration are the soil moisture and the surface albedo The soil moisture determines how large the evapotranspiration will be relative to the model calculated potential evapotranspiration (the evapotranspiration when soil moisture is fully available): the albedo is a major factor in determining the potential evapotranspiration itself.

The experiments that are being reviewed are grouped as follows:

  I. Experiments with non-interactive soil moisture.

  II. Experiments with interactive soil moisture.

  III. Hybrid experiments.

In the first group, either different soil moisture availabilities or different albedos are prescribed, and both of these parameters are kept constant with time. Such experiments reveal the sensitivity of the atmosphere to the boundary conditions. (These experiments are analagous to sensitivity experiments in which different non-interactive ocean surface temperatures are prescribed: the so-called sea surface temperature anomaly experiments).

In the second group, the soil moisture (but not the albedo) is interactive and changes with time according to the model's governing equations for soil moisture. When the albedos are the same in a pair of comparison runs, but the initial soil moistures are different, the integrations will either produce time-series that remain separate (intransitive) or converge to a common solution; and, if transitive, they will show how long it takes for the two initially different states to converge to a common state. When the albedos are different, this will be another kind of sensitivity experiment.

In the third group, the hybrid experiments, calculations with non-interactive and interactive soil moistures are compared. To the extent that the calculation with interactive soil moisture simulates the observed rainfall, temperature and circulation of the earth's atmosphere, the comparison will show how the earth's climate may be affected by such imposed changes in the land-surface evapotranspiration as might be brought about by large scale deforestation or afforestation, by soil erosion or reclamation, or by large scale irrigation.

LIST OF THE EXPERIMENTS

I. **Experiments with Non-Interactive Soil Moisture:**

    A. **Different soil moistures, with same albedo.**

        (1) Shukla and Mintz (1981).
        (2) Suarez and Arakawa (personal communication).
        (3) Miyakoda and Strickler (1981).

    B. **Different albedos, with same soil moisture.**

        (4) Charney, Quirk, Chow and Kornfield (1977).
        (5) Carson and Sangster (1981).

II. **Experiments with Interactive Soil Moisture:**

    A. **Different initial soil moistures, with same albedo.**

        (6) Walker and Rowntree (1977).
        (7) Rowntree and Bolton (1978).

    B. **Different albedos, with same initial soil moisture.**

        (8) Charney, Quirk, Chow and Kornfield (1977).
        (9) Chervin (1979).

III. **Hybrid Experiments:**

    Non-interactive vs. interactive soil moistures.

        (10) Manabe (1975).
        (11) Kurbatkin, Manabe and Hahn (1979).

I. EXPERIMENTS WITH NON-INTERACTIVE SOIL MOISTURE.

A. <u>Different Soil-Moistures, with Same Albedo.</u>

(1) <u>Shukla and Mintz (1981).</u>

The experiment of Shukla and Mintz (1981) used the general circulation model of the NASA Goddard Space Flight Center, Laboratory for Atmospheric Sciences. The properties of the GLAS model and its ability to simulate the regional and seasonal characteristics of the observed climate of the earth have been described by Shukla <u>et al.</u> (1981). In the experiment, one climate simulation is made in which the land-surface evapotranspiration, E, is everywhere made equal to the model calculated potential evapotranspiration, Ep, which makes the evapotranspiration coefficient, β = E/Ep = 1. In the other case, no land-surface evapotranspiration is allowed to take place at all (β = 0). The prescribed albedo is the same in both cases, and is a very slightly modified version of the one given by Posey and Clapp (1964). For convenience, the two calculations are called the "wet-soil" case and the "dry-soil" case. Both calculations were started from the same initial observed atmospheric state on 15 June. The results that are shown here are the averages for July.

In the wet-soil case, the calculated land-surface evapotranspiration is relatively constant (within about ± 1 mm/day) between latitudes 20°S and 60°N; with an average value of 4.3 mm/day; corresponding to an evaporative cooling of the surface of 125 watt/m², as shown in Fig. 2. Here, the sensible heat transfer to the atmosphere is 21 watt/m². In the dry-soil case, however, the land-surface evapotranspiration is zero and the sensible heat transfer is 169 watt/m².

The dry-soil case gives rise to much less cloudiness over the continents

| Wet-soil case | Dry-soil case |

$$R_L = (419\uparrow - 393\downarrow) = 26 \qquad R_L = (550\uparrow - 461\downarrow) = 89$$

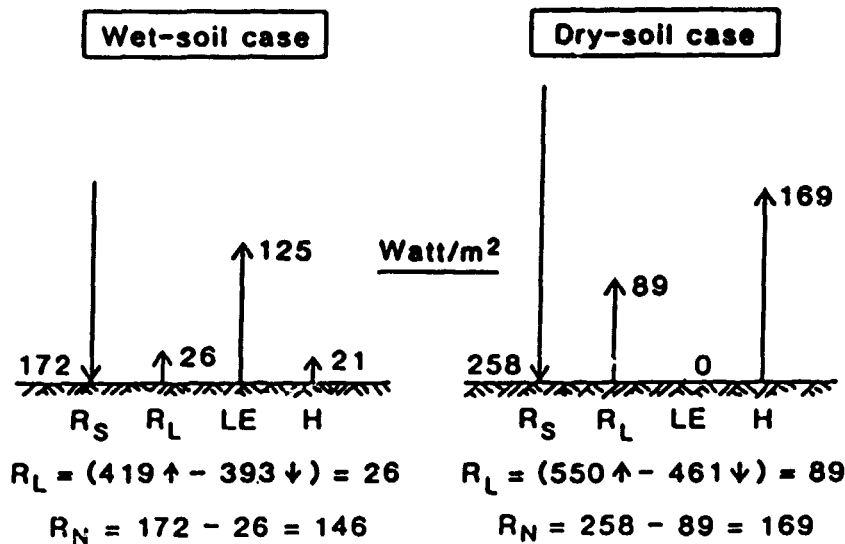$$R_N = 172 - 26 = 146 \qquad R_N = 258 - 89 = 169$$

Fig. 2 Surface energy transfers (watt/m^2) averaged for the continents between 20°S and 60°N, in experiment of Shukla and Mintz (1981).

R_S: solar radiational heating of the ground.

R_L: longwave radiational cooling of the ground (difference between radiation emitted by ground and radiation absorbed by ground.

$R_N = (R_S-R_L)$: net (all-wavlength) radiational heating of the ground.

LE: latent heat transfer from ground to atmosphere (evaporative cooling of the ground).

H : conductive-convective heat transfer from ground to atmosphere.

than the wet-soil case and, as a result, a larger amount of solar radiation
reaches and is absorbed by the ground, 258 instead of 172 watt/m^2. The
increased solar heating of the ground, as well as the elimination of the
evaporative cooling, makes the ground warmer; and the higher ground
temperature produces a greater long wave radiation emission from the ground,
550 instead of 419 watt/m^2. The atmosphere also becomes warmer in the
dry-soil case, and there is an increase in the atmospheric long wave "back
radiation" to the ground; but because of the reduction in the cloudiness
the increase in the back radiation, from 393 to 461 watt/m^2, is only
about half as large as the increase in the radiation emitted by the ground.
The end result of all these large, but partially compensating changes in
the radiation transfers, is that there is only a relatively small change
in the net (all-wavelength) radiational heating of the land-surface: an
increase of only 23 watt/m^2 from the wet-soil to the dry-soil case.

. 3   The top panel of Fig. 3 shows the global precipitation distribution in
the wet-soil case. Over most of North America and most of Eurasia the pre-
cipitation is with.. about 1 mm/day of the local evapotranspiration. Only
over southeast China does the precipitation exceed evapotranspiraton by as
much as 4 mm/day. Over South America there is heavy rain near the equator,
which is about 2 mm/day greater than the land-surface evapotranspiration.
Across Africa, at about 10°N, there is a band of rain which is about 4 mm/day
greater than the local evapotranspiration. On the other hand, across Africa
at about 25°N, and across Africa and South America at about 15°S, the precipi-
tation is 2 to 3 mm/day smaller than the evapotranspiration. Thus, although in
the wet-soil case there is a fairly uniform transfer of water vapor to the air
by the land-surface evapotranspiration, within the tropics and subtropics there
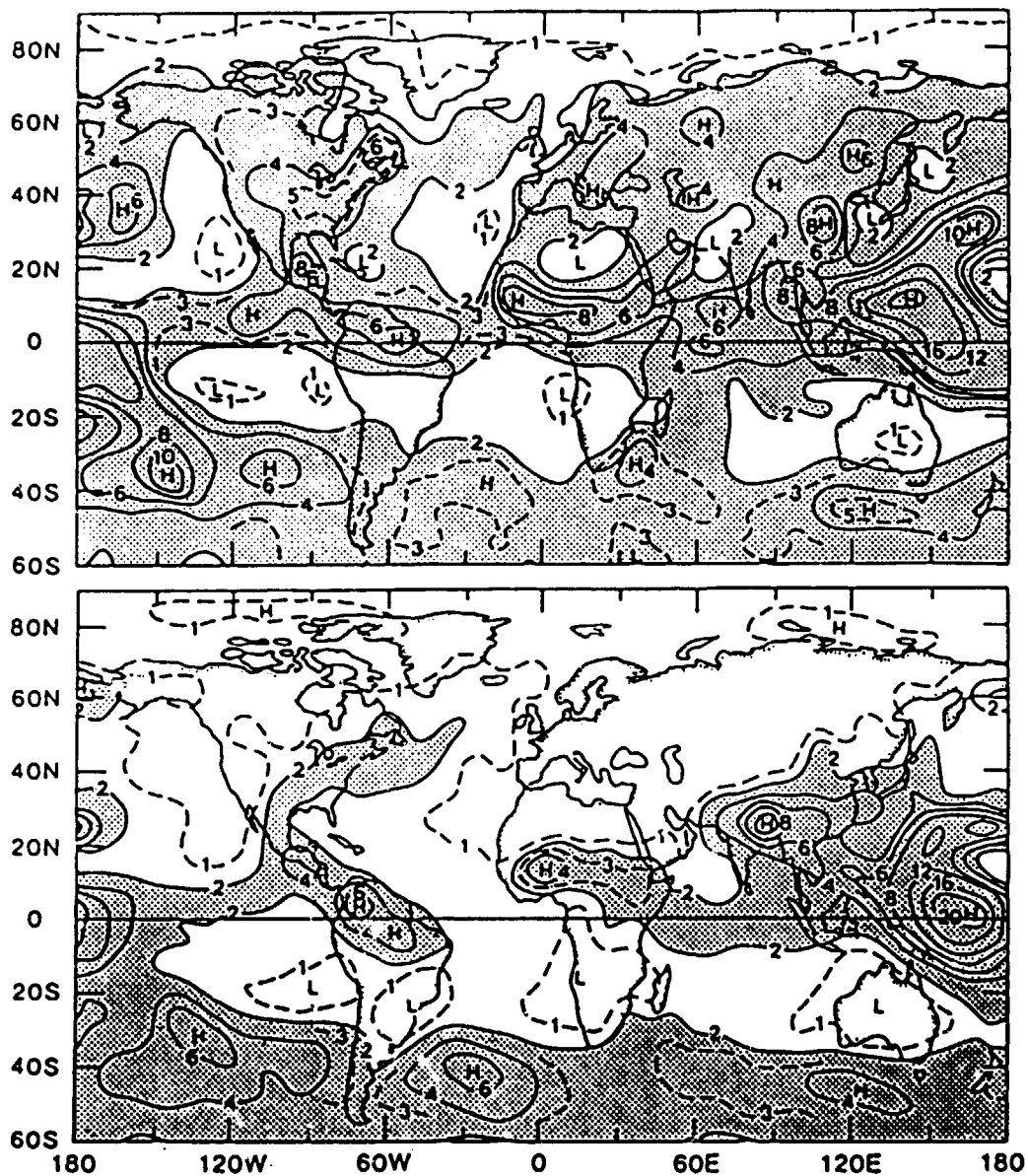are convergences and divergences of the water vapor transports by the large-

Fig. 3 Precipitation (mm/day) in wet-soil case (top) and dry-soil case (bottom), in experiment of Shukla and Mintz (1981). (Precipitation greater than 2 mm/day is shaded).

scale atmospheric circulation, which enhance or diminish the precipitation by substantial amounts.

The dry-soil case, shown in the bottom panel of Fig. 3, produces almost no precipitation at all over Europe and most of Asia; and over most of North America the precipitation is only about a quarter to a half of that of the wet-soil case. Over the equatorial part of South America, on the other hand, the rainfall in the dry-soil case is about the same as in the wet-soil case: i.e., about 6 mm/day; but, now, the water vapor which produces that precipitation comes only from the ocean.

Across north Africa, the rainband is about 400 km (one model grid interval) farther north in the dry-soil case than in the wet-soil case, and weaker by 3 to 4 mm/day. The precipitation in the dry-soil case is about the same as the amount by which the precipitation exceeded evapotranspiration in the wet-soil case: which is to say that the convergence of the water vapor transport by the atmospheric circulation is about the same in the two cases.

Perhaps the most surprising difference of all, when comparing the dry-soil case with the wet-soil case, is the southward and westward displacement of the region of maximum precipitation in southeast Asia. Over Bangladesh, the convergence in the water vapor transport from the ocean in the dry-soil case more than compensates for the absence of surface evapotranspiration. It is in the dry-soil case that the calculated precipitation most closely resembles the observed summer rainfall of southeast Asia.

ig. 4   Fig. 4 shows the ground surface temperature. In the dry-soil case, in which there is no evaporative cooling of the ground and, because of the reduced cloudiness, more solar radiation is absorbed by the ground, the surface temperatures north of latitude 20°S are about 15° to 30°C warmer than in the wet-soil case.
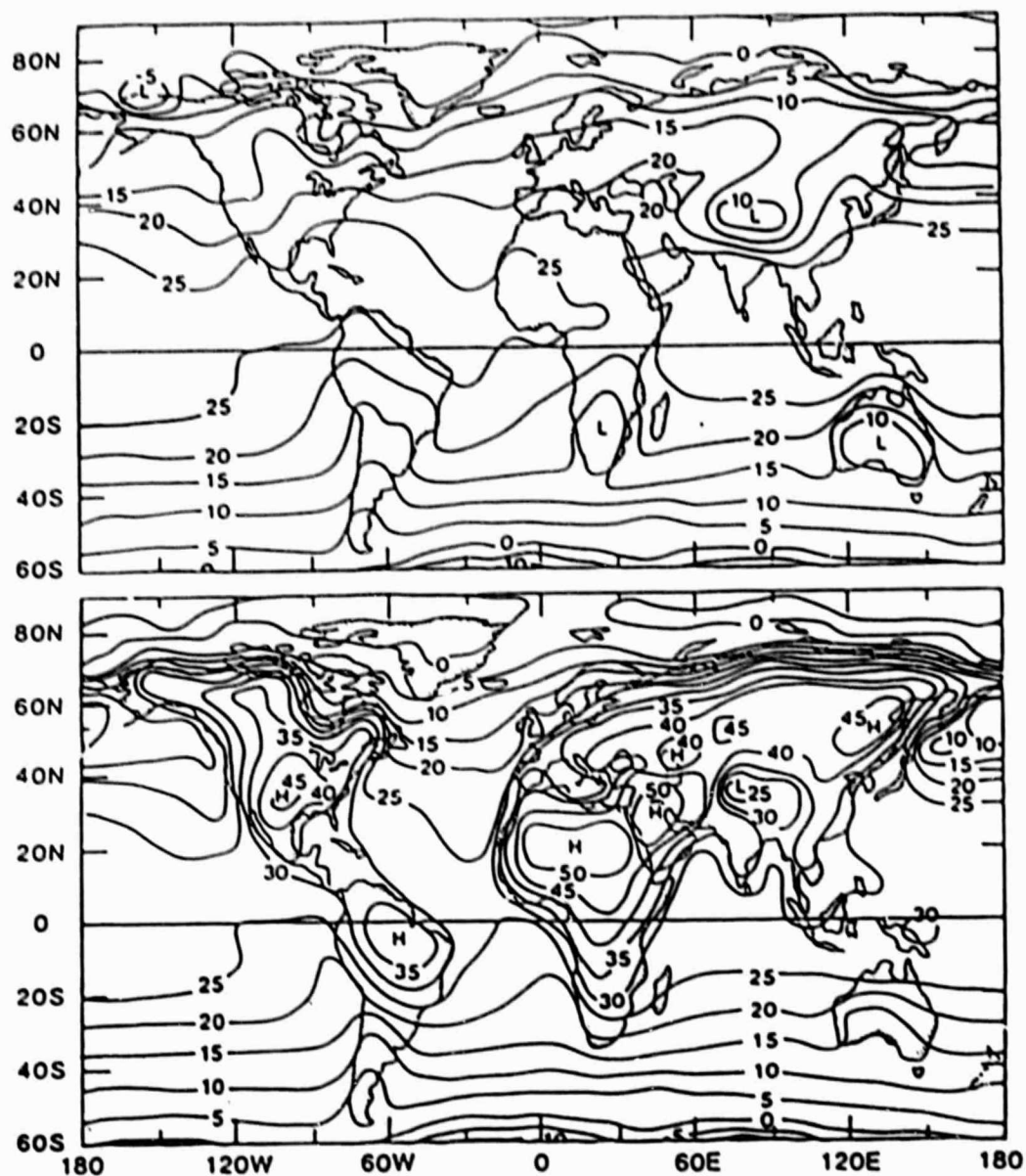
Fig. 4 Ground surface temperature (°C) in wet-soil case (top) and dry-soil case (bottom), in experiment of Shukla and Mintz (1981).

As shown in Fig. 2, the total non-radiational heat transfer to the atmosphere (H + LE) is not greatly different in the two cases (146 vs. 169 watt/m^2); but in the dry-soil case all of this is sensible heat transfer, which is confined to the planetary boundary layer. In the wet-soil case, by contrast, the larger part of the transfer is in the form of latent heat which warms the free atmosphere and not the boundary layer; whether immediately and locally realized by convective condensation and precipitation, or realized at some later time and distant place. Thus, there is a different vertical distribution, and sometimes a different horizontal distribution, of the diabatic heating. This can produce significant differences in the thermally forced atmospheric circulation and, by the geostrophic adjustment process, corresponding differences in the horizontal pressure distribution.
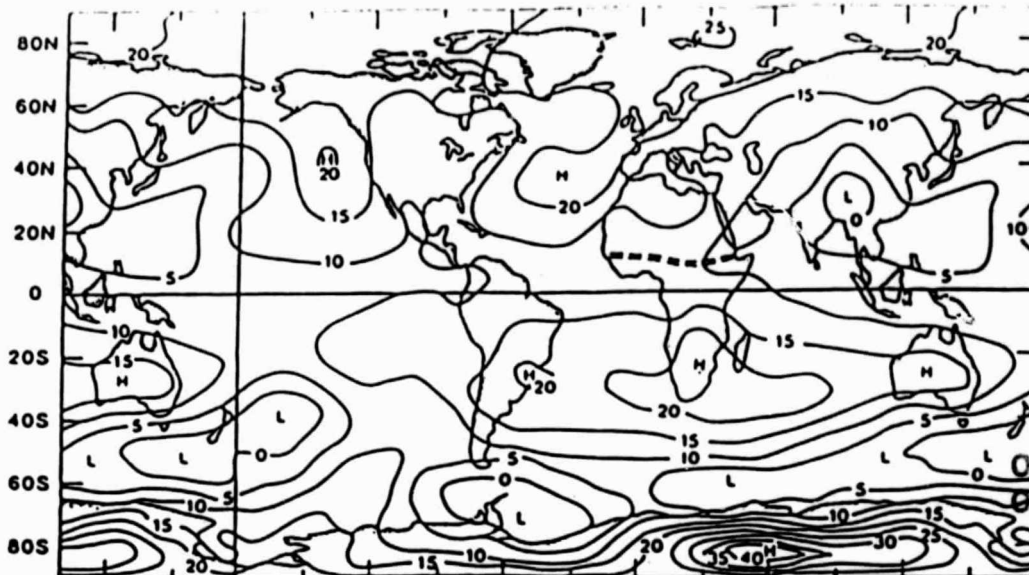
g. 5   Fig. 5 shows the surface pressure fields. The top and center panels show the surface pressures reduced to sea level, in the two cases. The bottom panel shows the difference between the two surface pressures, without reduction to sea level. It is here that we see the change in the surface geostrophic wind. Over most of the land the surface pressures are about 5 to 15 mb lower in the dry-soil case, which means enhanced cyclonic circulations over the continents.

In the wet-soil case the trough of low pressure across Africa coincides with the intertropical rainband, as may be seen by comparing the top panels of Figs. 3 and 5. This is the same relationship that we see over the tropical oceans. But in the dry-soil case the trough of low pressure is about 400 to 800 km north of the rainband; which is about the same relationship that is found over north Africa, in nature.

When the surface pressure is lower over the continents, it must be higher over the oceans. Most of the increase is in the mid-latitudes of the central
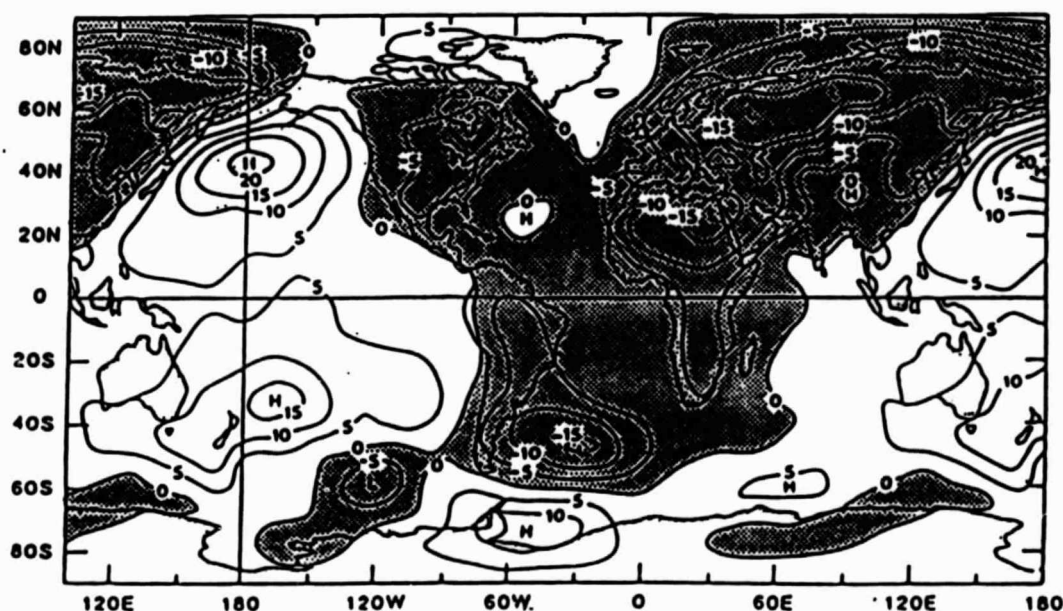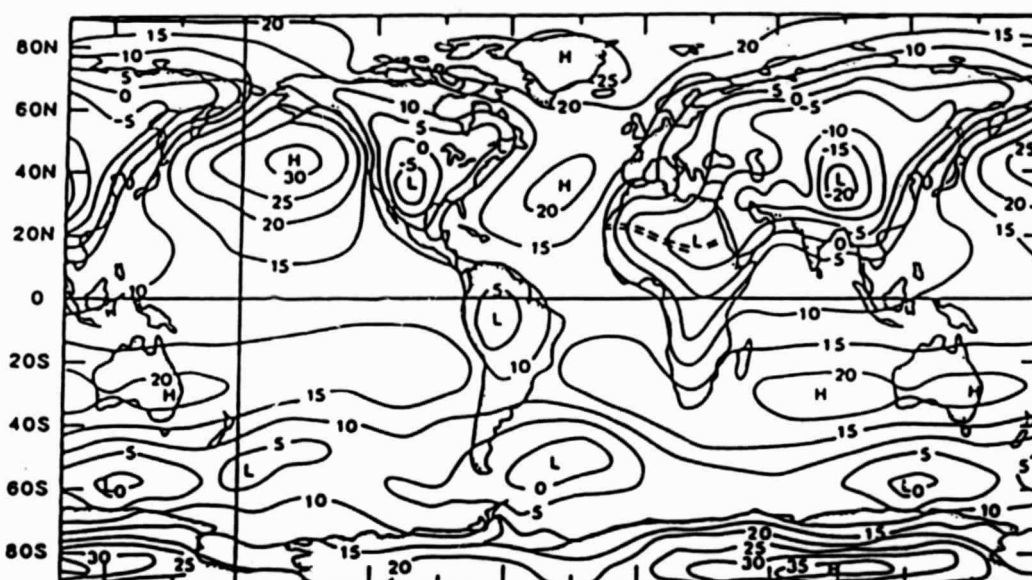
-12-

Fig. 5   Surface pressure reduced to sea level (mb minus 1000) in wet-soil case (top) and dry-soil case (center), in experiment of Shukla and Mintz (1981).   Bottom map shows the difference between the two surface pressures (mb).

and western North and South Pacific Oceans. Examination of the vertical motion field (not reproduced here) shows that in these ocean regions there is an increased subsiding motion in the dry-soil case. As Figs. 3 and 5 show, not only does the increased sinking motion suppress the oceanic precipitation, but the accompanying low-level horizontal velocity divergence, by generating anticyclonic vorticity, increases the anticyclonic circulation in these regions; and geostrophic adjustment produces the corresponding rise in surface pressure.

Over the Atlantic Ocean, the vertical motion field in the wet-soil case shows a band of rising motion and low-level velocity convergence, which coincides with the band of oceanic precipitation just north of the equator (top panel of Fig. 3). But in the dry-soil case there is sinking motion over all of the tropical Atlantic; and there is no oceanic rainband near the equator at all. Over the eastern half of the tropical Pacific, the same kind of change takes place, but it is not as pronounced. Thus, the change in the land-surface boundary condition also produces large changes in the circulation and rainfall over the oceans.

(2) Suarez and Arakawa (personal communication).

At the reviewer's suggestion, the same wet-soil (β=0) versus dry-soil
(β=1) sensitivity experiment was made with the UCLA general circulation model
by M. Suarez and A. Arakawa (personal communication). (For a
description of the model, see Arakawa and Lamb, 1977; Arakawa and Suarez,
1983; and Suarez et al., 1983.) There are substantial differences between
the UCLA and the GLAS models, of which the most important, insofar as the
present sensitivity experiment is concerned, may be the way in which the
planetary boundary layer and the cumulus convection are parameterized.

In the UCLA experiment the integrations for the two cases were started on
the first day of July, with the initial state of the atmosphere taken from a
previous general circulation simulation. The results that are shown here are
for the 31-day period starting on 16 July. Again, the prescribed surface
albedo follows Posey and Clapp (1964).

In the wet-soil case, the calculated land-surface evapotranspiration was
relatively constant (within about ± 1 mm/day) between 20°S and 60°N, with an
average value of about 6 mm/day. This is about 1.7 mm/day larger than in the
wet-soil case of the GLAS experiment, and is probably a consequence of the fact
that the UCLA model produces less cloud cover than does the scheme used in
the GLAS model and, thereby, a greater net radiational heating of the ground.

g. 6   Fig. 6 shows that the precipitation in the wet-soil case is about
6 ± 1 mm/day, over almost all of extratropical North America and Eurasia, and,
therefore, does not differ from the local evapotranspiration by more than about
1 mm/day. Within the tropics, however, the precipitation exceeds the local
evapotranspiration by about 10 mm/day over the Indochina peninsula, by about
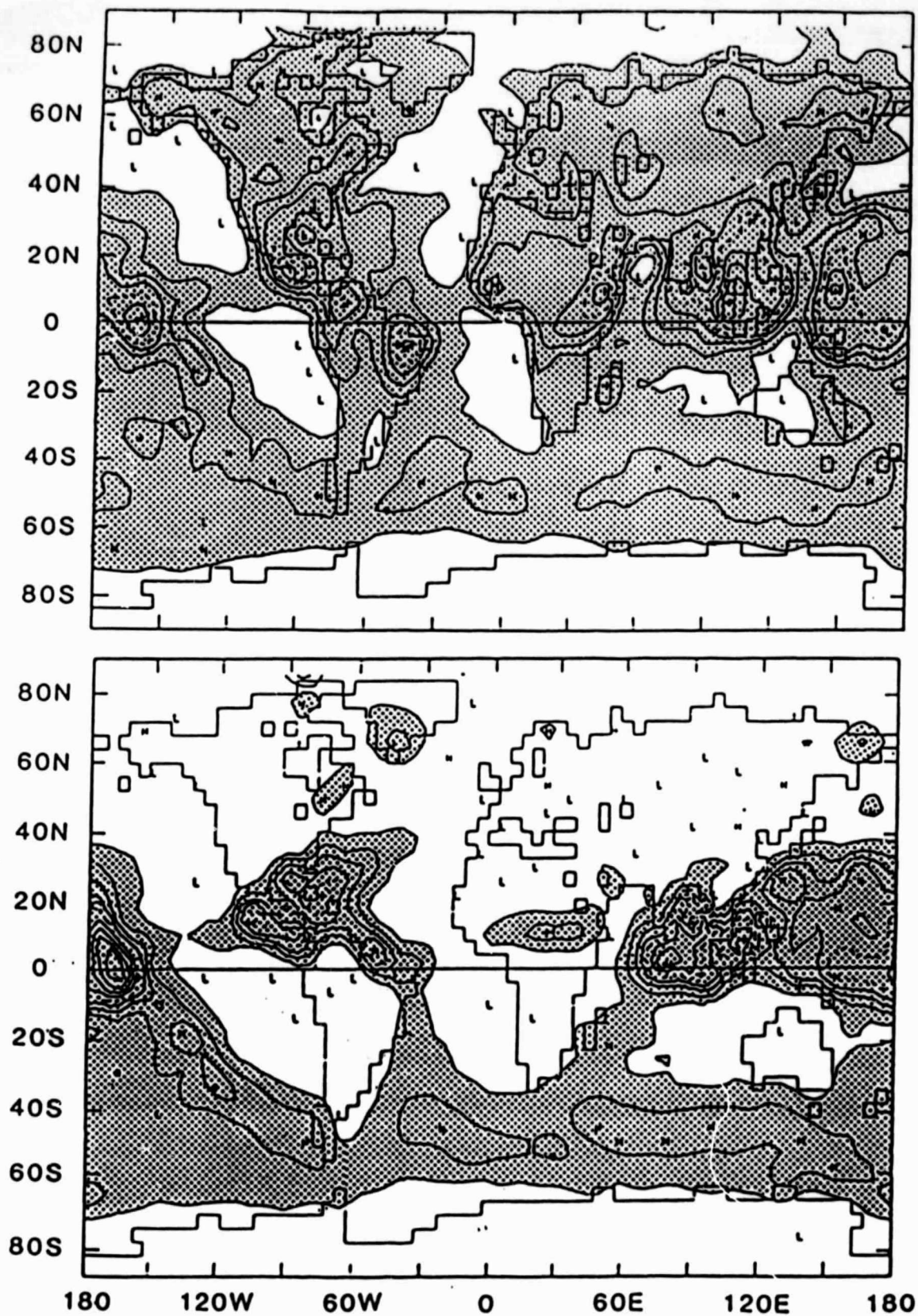3 to 6 mm/day over a few small land areas that are close to the sea (Guatemala,

Fig. 6   Precipitation (mm/day) in the wet-soil case (top) and dry-soil case (bottom), in the experiment of Suárez and Arakawa (personal communication). (Precipitation greater than 2 mm/day shaded).

southern India, southeast China, Columbia, Venezuela and northeast Brazil),
and by a few mm/day over a large area adjacent to the Somali coast of
north Africa. These are regions, therefore, of substantial water vapor
transport convergences.

In the dry-soil case, shown in the bottom panel of Fig. 6, there is
almost no continental precipitation at all. Only in an east-west band across
north Africa is there a significant amount of precipitation, 2 to 5 mm/day,
produced by a convergence of the water vapor transported from the oceans. The
axis of this rainband, at 10°N, is about 1000 km south of the axis of the low
pressure trough which, in the dry-soil case, is at about 20°N.

The change in the precipitation over the oceans is very large near some
of the tropical and subtropical coastlines, and especially where there are
embayments. In the wet-soil case there are pronounced minima over the Gulf of
Mexico and the Bay of Bengal (accompanied by pronounced maxima over the adja-
cent land areas). But in the dry-soil case, the minima are replaced by maxima
over the ocean embayments. Similarly, along the coasts of Central America and
northeast Brazil, the land precipitation decreases and the nearshore ocean
precipitation increases in going from the wet-soil to the dry-soil case.

The striking difference between the experiments with the UCLA model and
the GLAS model is that, except for the Sahel region of Africa, the UCLA
model produces almost no continental precipitation in the dry-soil case.

Examination of the water vapor transport field by the investigators showed
that there are regions, such as northeast Brazil, where within the planetary
boundary layer there is a large convergence of the water vapor transported from
the ocean, in the dry-soil case, but no rain. The interpretation they made
(Suarez and Arakawa, personal communication) is that with dry-soil there is a
very large diurnal variation of the ground surface temperature, which produces

a very large diurnal variation in the depth of the model's planetary boundary layer, growing in thickness during the day and collapsing at sunset; and that it is this diurnal oscillation which, without producing clouds, transfers the water vapor from the boundary layer to the free atmosphere, where the transport is divergent. This transfer of water vapor from the boundary layer to the free atmosphere by diurnal "boundary layer/free atmosphere mixing" is not unlike the transfer by detrainment from fair-weather, non-precipitating cumulus clouds, described in the introduction. The same condition of upper troposphere velocity convergence and middle troposphere subsidence must be satisfied. Here it is the result of upper level outflow from the region of intense convective precipitation over the adjacent ocean.

(3) Miyakoda and Strickler (1981).

Miyakoda and Strickler (1981) used an early version of the general
circulation model of the NOAA/Princeton Geophysical Fluid Dynamics Laboratory
(Miyakoda et al., 1969) to make and compare two different sets of 14 day
numerical weather predictions for the northern hemisphere, in July, when diffe-
rent distributions of the soil moisture availability, β, were prescribed.

The surface albedo was fixed and followed Posey and Clapp (1964). The
clouds were climatologically prescribed as a function of latitude and height.
The convective-adjustment scheme was used, in which the moist convective
heating of the atmosphere and the convective precipitation depend only on the
relative humidity and on the temperature difference between adjacent levels in
the vertical. Thus there is no penetrative convection and, consequently, the
sensitivity of the convective heating and precipitation to the amount of water
vapor in the model's planetary boundary layer is not as great as in the cumulus
convection parameterization schemes of the GLAS and the UCLA models.

In one case β was everywhere set equal to 0.5. For the other case, the
authors sought a more realistic field of β; and for this they took the ob-
served normal distribution of precipitation for the antecedent six month
period, February through July, and relabeled the isohyets as lines of constant
β, according to the arbitrary function shown in the top panel of Fig. 7
(Miyakoda et al., 1979). No account was taken of the antecedent evapotranspira-
tion. Consequently, as the bottom panel of the figure shows, over the northern
forests and the wet tundra regions of Canada and Siberia β was made as low as
in the subtropical deserts (although, in nature, it is near the maximum value
of 1.0).

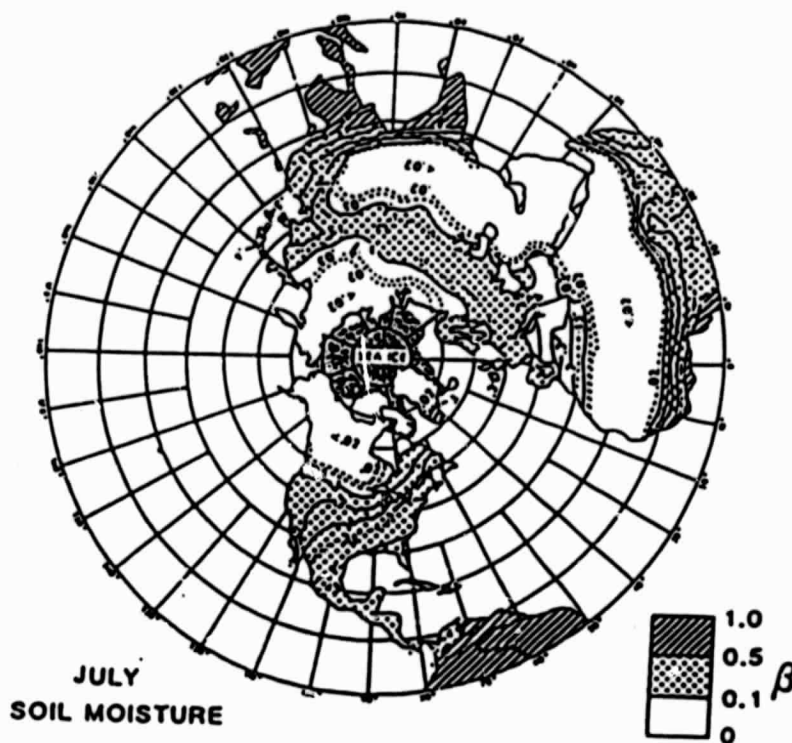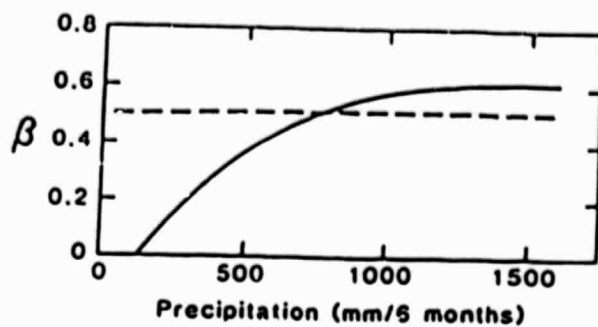Figures 8 and 9 show the differences in the evapotranspiration, precipita-

Fig. 7   Soil moisture availability, β, in July, as derived from antecedent 6 month precipitation (Miyakoda, *et al.*, 1979).

$\beta = \beta(\lambda,\phi)$ minus the case of $\beta \equiv 0.5$, when the ensemble average is taken of the last twelve days of three sets of 14-day forecasts.

Fig. 8   We see, in Fig. 8, that where β is reduced there is, in general, a reduction in evapotranspiration and precipitation. The largest reduction in evapotranspiration, of more than 7 mm/day, is over the central part of the north African and Asian deserts; with the axis of the maximum evapotranspiration reduction at about latitude 20°N across Africa. But the axis of the largest reduction in precipitation is at about 12°N across Africa (the Sahel), where the precipitation decreases by about 12 mm/day. As shown in Miyakoda and Strickler (1981, Fig. 7), the rainband of the intertropical convergence zone across north Africa does not change its position, but its magnitude goes down from about 20 to 8 mm/day when the land-surface moisture source in the Sahara is eliminated. There is, obviously, a large change that takes place in the water vapor transport.

In the case where the average land-surface evapotranspiration became smaller, the average ocean evaporation become larger. In spite of that, the average ocean precipitation decreased, in agreement with the experiments made with the GLAS and UCLA models. Presumably it is, again, an enhancement of the sinking motion over the oceans that suppresses the ocean precipitation.

Fig. 9   If we compare the top panel of Fig. 9 with the top panel of Fig. 8, we see that there is a negative correlation between the change in the land-surface temperature and the change in evapotranspiration.

When we compare the upper and lower panels of Fig. 9, we see that there is a negative correlation between the change in surface temperature and the change in the height of the 1000 mb surface. This is true even where the land-surface is not at a high elevation.

This experiment shows two important things: 1) That it does not require

EVAP DIFFERENCE
SOIL MOIST EXP. – CONTROL EXP.

PRECIP DIFFERENCE
SOIL MOIST EXP. – CONTROL EXP.

Fig. 8   Evapotranspiration difference (top) and precipitation difference
(bottom), when $\beta \equiv 0.5$ is replaced by $\beta(\lambda,\psi)$, in experiment of Miyakoda and
Strickler (1981). (Contours for 0, ∓ 25, ∓ 100, ∓ 200, ∓ 500 mm/mo. Negative
values shaded).

SURFACE TEMP. DIFF.
SOIL MOIST EXP. - CONTROL EXP.

1000mb HGT. DIFF.
SOIL MOIST EXP. - CONTROL EXP.

Fig. 9 Surface temperature difference (top) (contour interval 2.5°C) and difference in height of the 1000 mb surface (bottom) (contour interval 10 m; negative values shaded), in experiment of Miyakoda and Strickler (1981).

an extreme change in the soil moisture availability (β), such as a change from 1 to 0, in order to produce large changes in the precipitation, temperature and motion fields. And, 2) that the influence of the land-surface evapotranspiration on the atmosphere operates very quickly. Miyakoda (personal communication) reports that sizeable differences in the surface temperature and precipitation appeared within a few days.

[In an earlier study of the role of the surface transfers of sensible and latent heat in numerical weather prediction, Gadd and Keers (1970, Figs. 4, 5, 6) showed that even in a very short range (18-hour) prediction for north-western Europe and the British Isles, in August, the inclusion of evaporation and sensible heat transfer from   the land and the sea surfaces made a noticeable improvement in the predicted rainfall over the land].

B. Different Albedos, with Same Soil Moisture.

(4) Charney, Quirk, Chow and Kornfield (1977).

This experiment was made by Charney et al. (1977) with the NASA Goddard Institute for Space Studies general circulation model, the properties and performance of which have been described by Somerville et al. (1974) and Stone et al. (1977).

The three runs that are shown here use the prescribed field of non-interactive soil moisture availability, β, from Stone et al. (1977), who assumed that $\beta = 2 \times (RH - 15)/85$, $\beta_{max} = 1$, where RH is the observed normal monthly mean relative humidity of the surface air. The observed relative humidities, for July, were taken from the tabulation by Schutz and Gates (1972). In the above formulation, $\beta = 1$ when the relative humidity is equal to or greater than 57.5%. Consequently, β was made equal to or close to 1, and the evapotranspiration therefore equal to or close to the potential evapotranspiration over most of the land surface of the earth. Only in a small region in the western United States and across the central Sahara was the prescribed July β smaller than 0.5.

In the run designated as case "2a", the ice-free and snow-free continents were assigned a surface albedo of 0.14; except that a higher albedo, 0.35, was assigned to the regions of the observed northern hemisphere deserts (see Fig. 19, below).

In a comparison run, "3a", the albedo was changed from 0.14 to 0.35 in three additional regions, the "Sahel", "Rajputana", and "Western Great Plains", which are adjacent to deserts (Fig. 19). Otherwise everything was the same as in case 2a.

In a separate comparison run, case "4", everything was again the same

-20-

as in case 2a, except that the change of albedo, from 0.14 to 0.35, was

made in three regions that are within the observed rainy and vegetation

covered areas of the earth. The locations of these regions, called "Central

Africa", "Bangladesh", and "Mississippi Valley" are given in the table.

The first numbered column of Table I shows the prescribed soil mois-

ture availabilities for the six regions. In the Sahel region $\beta = 0.51$, and

in the other regions β is 0.78 or more.

Fig. 10   Fig. 10 shows the evapotranspiration and precipitation in the northern

hemisphere, for case 3a. Over most of the continents the evapotranspiration

and precipitation do not differ by more than about ± 1 mm/day. It is only

over southeast China and Indochina, and where the intertropical rainband

crosses Africa, that the precipitation exceeds the evapotranspiration by

3 to 4 mm/day. Near the Mediterranean coast of Africa and in the Middle East

the precipitation is less than the evapotranspiration by about 2 to 4 mm/day.

Table I   Table I is a rearrangement of the data in Charney et al. (1977, Tables

4.1 to 4.4) and shows the components of the energy and water budgets at the

earth's surface in the three desert-margin regions, (case 2a vs. 3a) and in

the three humid regions (case 2a vs. 4).

We see, in column (10), that in the Western Great Plains (where β was

assigned the value of 0.78) and in the Mississippi Valley (where β was made

1.0), the evapotranspirations with albedo of 0.14, are, respectively, 4.2

mm/day (130 mm/mo) and 5.1 mm/day (158 mm/mo). These are in fair agreement

with the aerologically derived evapotranspiration over the central and

eastern United States in July, of 3.7 mm/day (116 mm/mo), shown in Fig. 1.

More important, however, as an indication of the reliability of the model,

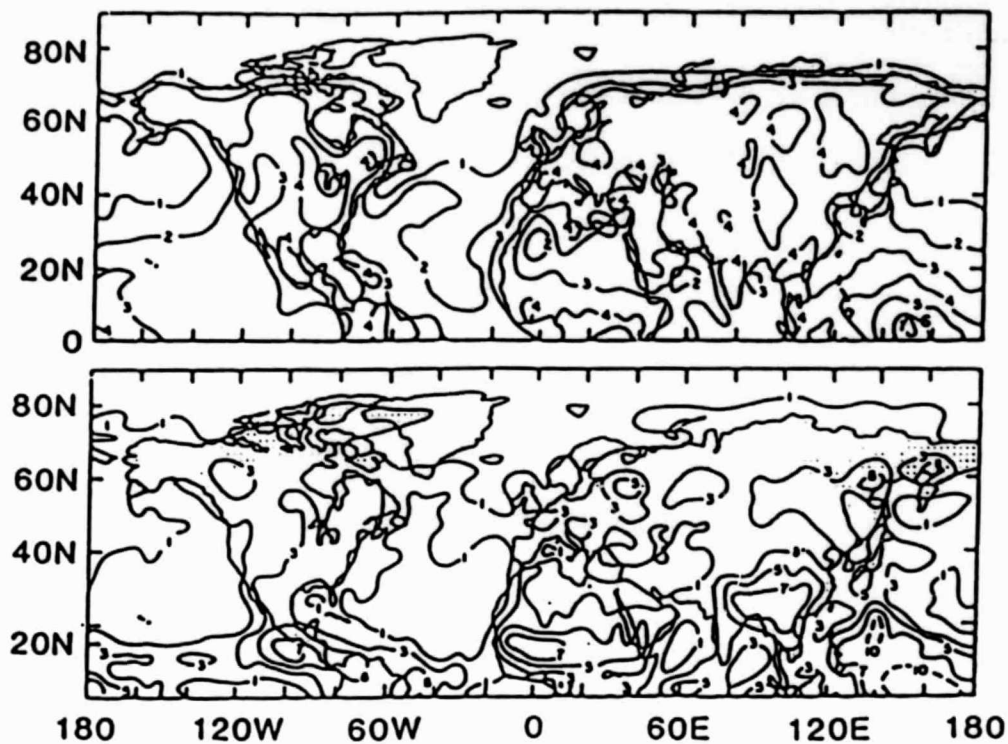is the fact that the vertical integral of the water vapor flux convergence,

Fig. 10   Evapotranspiration (top) and precipitation (bottom) (mm/day),
in experiment with prescribed soil moisture availability (case 3a) of
Charney et al. (1977).

Table I. Components of the energy and water budgets, in experiment of Charney et al. (1977)

Region	Case No.	(1) β	(2) (1-α)	(3) Rs	(4) RL	Energy Balance (5) RN	(6) LE	(7) H	(8) N	(9) TA	Water Balance (10) E	(11) (-∇·qv)	(12) P	(13) Δ(-∇·qv)/ΔE	(14) ΔP/ΔE
1. Sahel (16°N–20°N, 17.5°W–37.5°E)	2a	0.51	0.86	169	58	111	107	4	0.70	26.0	3.7	3.7	7.4		
	3a	0.51	0.65	177	84	93	81	12	0.46	25.7	2.8	1.2	4.0		
			−24%	+5%	+49%	−18	−26	+8	−34%	−0.3	−0.9	−2.5	−3.4	2.8	3.8
2. Rajputana (24°N–32°N, 67.5°E–77.5°E)	2a	0.92	0.86	180	48	132	119	13	0.77	24.9	4.1	0.8	4.9		
	3a	0.92	0.65	189	75	114	104	10	0.57	24.1	3.6	−1.3	2.3		
			−24%	+5%	+56%	−18	−15	−3	−26%	−0.8	−0.5	−2.1	−2.6	4.2	5.2
3. Western Great Plains (32°N–48°N, 107.5°W–97.5°W)	2a	0.78	0.86	186	62	124	122	2	0.67	21.1	4.2	−0.5	3.7		
	3a	0.78	0.65	185	79	106	93	13	0.52	19.0	3.2	−1.0	2.2		
			−24%	+1%	+27%	−18	−29	+11	−22%	−2.1	−1.0	−0.5	−1.5	0.5	1.5
4. Central Africa (8°N–12°N, 12.5°W–52.5°E)	2a	0.94	0.86	170	56	114	125	−11	0.72	22.2	4.3	0.7	5.0		
	4	0.94	0.65	171	69	102	104	−2	0.59	21.6	3.6	−1.7	1.9		
			−24%	+1%	+23%	−12	−21	+9	−18%	−0.6	−0.7	−2.4	−3.1	3.4	4.4
5. Bangladesh (20°N–28°N, 77.5°E–87.5°E)	2a	1.00	0.86	149	38	111	113	−2	0.85	24.2	3.9	4.1	8.0		
	4	1.00	0.65	140	44	96	107	−11	0.78	23.6	3.7	4.3	8.0		
			−24%	−6%	+16%	−15	−6	−9	−8%	−0.6	−0.2	0.2	0	−1.0	0.0
6. Mississippi Valley (32°N–48°N, 92.5°W–82.5°W)	2a	1.00	0.86	208	68	140	148	−8	0.57	22.1	5.1	−0.7	4.4		
	4	1.00	0.65	170	67	103	102	1	0.56	22.6	3.5	−0.2	3.3		
			−24%	−18%	−1%	−37	−4.6	+9	−2%	+0.5	−1.6	+0.5	−1.1	−0.3	0.7
Average for the six regions		0.86	0.86	177	55	122	122	0	0.71	23.4	4.2	1.4	5.6		
		0.86	0.65	172	70	102	98	4	0.58	22.8	3.4	0.2	3.6		
			−24%	−3%	+27%	−20	−24	+4	−18%	−0.6	−0.8	−1.2	−2.0	1.5	2.5

β :   average, for the region, of the prescribed soil moisture availability (ratio of evapotranspiration to potential evapotranspiration)

$(1 - \alpha)$:   fraction of the incident solar radiation that is absorbed by the ground (α = land-surface albedo)

R_S :   solar radiational heating of the ground (watt/m^2)

R_L :   longwave (infrared) radiational cooling of the ground (difference between longwave radiation emitted by the ground and atmospheric "back radiation" absorbed by the ground) (watt/m^2)

$R_N = (R_S - R_L)$:   net (all-wavelength) radiational heating of the ground (watt/m^2)

LE :   latent heat transfer from ground to atmosphere (evaporative cooling of the ground)

H :   conductive-convective heat transfer from ground to atmosphere

N :   fraction of the sky covered by clouds of all types

T_A :   surface air temperature ($^\circ$C)

E :   surface evapotranspiration (mm/day)

$(-\overline{\nabla \cdot q\, \mathbf{v}})$:   vertically integrated convergence of the water vapor transport (mm/day)

P :   precipitation (mm/day)

$\Delta P/\Delta E$. :   ratio of precipitation change to evapotranspiration change

For each region the third line shows either the absolute change between the two cases or the percentage change, where the % sign indicates the latter.

$(-\overline{\nabla \cdot q \, w})$, shown in column (11), is negative in the two regions,
with values respectively of -0.5 mm/day (-16 mm/mo) and -0.7 mm/day
(-22 mm/mo). This means that water vapor is being exported from these re-
gions at about the same rate as the observed transport divergence, of
0.7 mm/day (22 mm/mo), shown in Fig. 1.

In the other four regions, in the case with normal surface albedo, 2a,
the vertical integrals of the water vapor transport convergence are positive,
water vapor is being imported (so that precipitation is larger than evapotran-
spiration), which is what one would expect for these particular regions in
the month of July.

Table I is replete with information about the performance of the model
and its complex, non-linear response to the change in the surface albedo. But,
for brevity, we will here examine only what happens in the Sahel, the region
of greatest interest.

Fig. 11   We see, in Table I (column 3), and in Fig. 11, that when the surface
albedo is increased in the Sahel, from 0.14 to 0.35, the solar radiational
heating of the surface does not become smaller: it becomes larger. This is
because of the large decrease in the cloud cover, from 0.70 to 0.46, (column
8), which more than compensates for the increased albedo.

The cloud cover is less because 1) there is less evapotranspiration
(a change from 3.7 to 2.8 mm/day), and 2) there is less convergence in the
water vapor transport (a change from 3.7 to 1.2 mm/day).

The local evapotranspiration is reduced in the high-albedo case because
there is more long wave radiational cooling of the ground (an increase from
58 to 84 watt/m^2). Unfortunately, no record was kept of the ground surface
temperature, nor of the long wave emission by the ground; but it is most
likely that it is the decrease in the downward longwave "back radiation" from
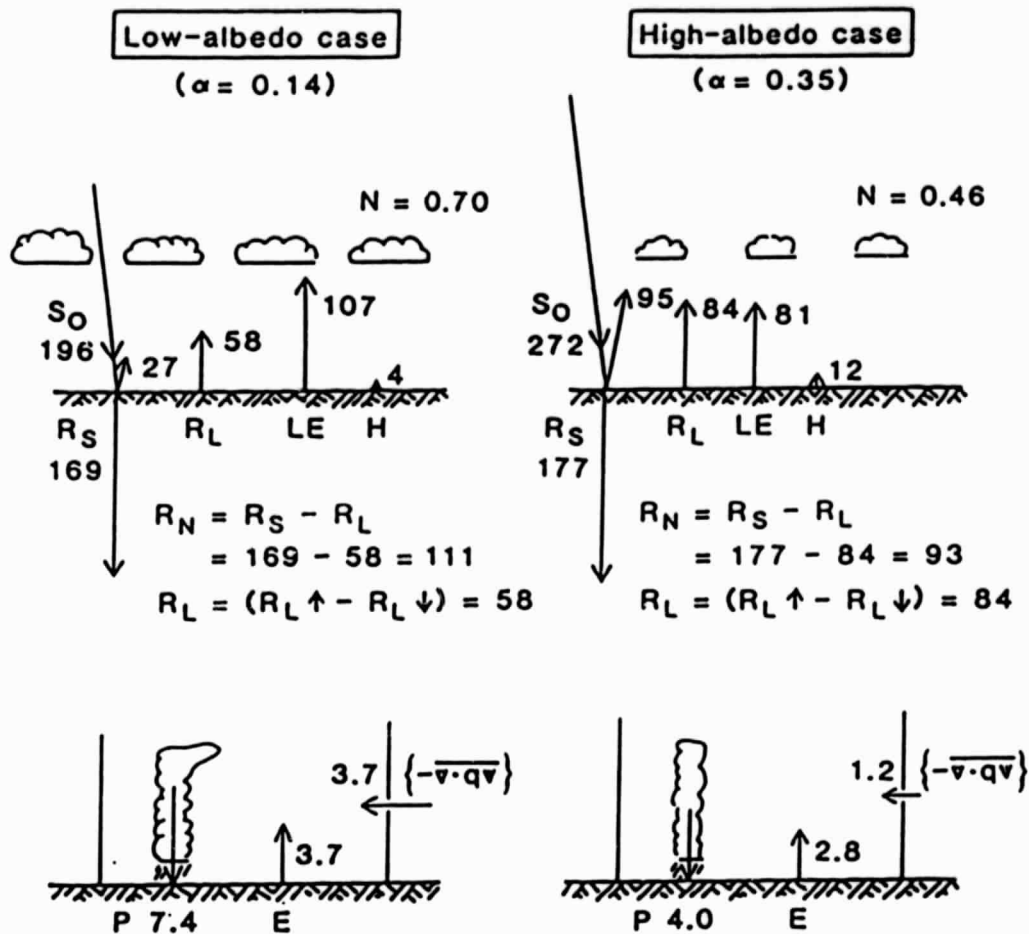
-23-

| Low-albedo case | High-albedo case |
| $(\alpha = 0.14)$ | $(\alpha = 0.35)$ |

N = 0.70

N = 0.46

S_O
196

27   58   107

4

R_S R_L LE   H

169

S_O
272

95   84   81

12

R_S R_L LE   H

177

$R_N = R_S - R_L$
$= 169 - 58 = 111$
$R_L = (R_L\uparrow - R_L\downarrow) = 58$

$R_N = R_S - R_L$
$= 177 - 84 = 93$
$R_L = (R_L\uparrow - R_L\downarrow) = 84$

3.7 $\{-\overline{v}\cdot q\overline{v}\}$

3.7

P 7.4   E

1.2 $\{-\overline{v}\cdot q\overline{v}\}$

2.8

P 4.0   E

Fig. 11   The Sahel region energy budgets (watt/m²) (top) and water budgets (mm/day) (bottom), in the experiment with prescribed soil moisture availability of Charney et al. (1977). Case 2a is on the left, Case 3a is on the right. (For definitions of symbols, see legend of Table I).

the atmosphere, $R_L\!\downarrow$, as a consequence of the decreased cloudiness, which increased the long wave cooling of the ground.

The sensible heat transfer from the ground to the atmosphere is small, in both cases.

By using arrows to indicate when a change in one parameter produces a change in another, we can describe what happens in the Sahel, in this experiment, as the coupling between a sequence of processes operating locally and a sequence that involves the large scale atmospheric circulation. The local sequence is: albedo $\xrightarrow{\text{(changes)}}$ radiation $\xrightarrow{\text{(changes)}}$ evapotranspiration $\xrightarrow{\text{(changes)}}$ precipitation. The larger scale sequence is: precipitation/condensation-heating $\xrightarrow{\text{(changes)}}$ large scale circulation $\xrightarrow{\text{(changes)}}$ water vapor transport convergence $\xrightarrow{\text{(changes)}}$ precipitation.

The second of these two sequences is similar (but not identical) to the one in the Charney (1975) hypothesis on the dynamics of deserts. In that hypothesis the sequence is: albedo $\xrightarrow{\text{(changes)}}$ surface temperature $\xrightarrow{\text{(changes)}}$ large scale circulation $\xrightarrow{\text{(changes)}}$ water vapor transport convergence $\xrightarrow{\text{(changes)}}$ precipitation. Here, the change in evapotranspiration plays no role. [A direct examination of the Charney (1975) hypothesis with a general circulation model would consist of a comparison of two runs, in both of which no evapotranspiration is allowed in the region of interest, but is allowed elsewhere, and the albedo in the region of interest is changed]. [See experiment (8), below.]

The relative importance of the two sequences of processes, when surface evapotranspiration does take place, may be seen in columns (13) and (14) of Table I. We see, in column (13), that in the Sahel, Rajputana and Central Africa, the reduction in the water vapor flux convergence is between 2.8 to 4.2 times larger than the reduction in the evapotranspiration. But in the

Western Great Plains the reduction in the water vapor flux convergence is only half as large as the reduction in evapotranspiration. In Bangladesh and the Mississippi Valley things go the other way: increasing the surface albedo again decreases the evapotranspiration; but it _increases_ the water vapor flux convergence.

As indicated earlier, the response of the large scale precipitation, temperature and motion fields to a change in the surface boundary conditions (whether soil moisture availability or albedo) will depend on many factors. Of particular importance is the horizontal scale and the latitude of the region in which the boundary condition is changed. Through the geostrophic adjustment process, the horizontal scale and the latitude determine whether the circulation change will be in the vertical plane (small scale or low latitude) or in the horizontal plane (large scale and high latitude). When the circulation change is in the vertical plane there is a positive feedback on the condensation hea. g, through water vapor transport convergence. But when the circulation change is in the horizontal plane there is a negative feedback on the condensation heating, because then the transport removes water vapor, as well as sensible heat, from the region of the condensation heating.

(5) <u>Carson and Sangster</u> (1981).

Another experiment in this category was made by Carson and Sangster (1981) with a low resolution (N20) version of the British Meteorological Office 5-layer general circulation model (Corby <u>et al.</u>, 1977). In both runs, evapotranspiration was made equal to the calculated potential evapotranspiration, ($\beta \equiv 1$). In one case the albedo of the snow-free land was everywhere set equal to 0.1. In the other case, it was everywhere set equal to 0.3. The remaining lower boundary conditions (sea surface temperatures, sea ice, and land snow cover), as well as the climatologically determined longwave radiational heating rates, were the observed July values.

<u>Fig. 12</u>   Figure 12 shows the precipitation averaged over 90 days (Days 21 to 110 of integration), where the top panel is the low albedo case, the center panel is the high-albedo case, and the bottom panel is the difference between the two.

We see that the high albedo case has less rainfall over most of the continental areas; but that over the oceans the rainfall is increased.

The averages of the land precipitation,, and of other parameters, are

<u>Table II</u>   shown in Table II.

Like the experiment by Charney <u>et al.</u>, (4) above, this is also an albedo change experiment with permanently wet-soil ($\beta \equiv 1$). Here, too, the increase of albedo produced a decrease in evapotranspiration (-0.9 mm/day) and an even larger decrease in precipitation (-1.2 mm/day); but now the albedo is changed on the continental scale, whereas in (4) it was changed on a scale of only a few hundred kilometers in the widths of the various regions. It is not surprising, therefore, that in this experiment the contribution to the change in precipitation of the change in the water vapor transport convergence is
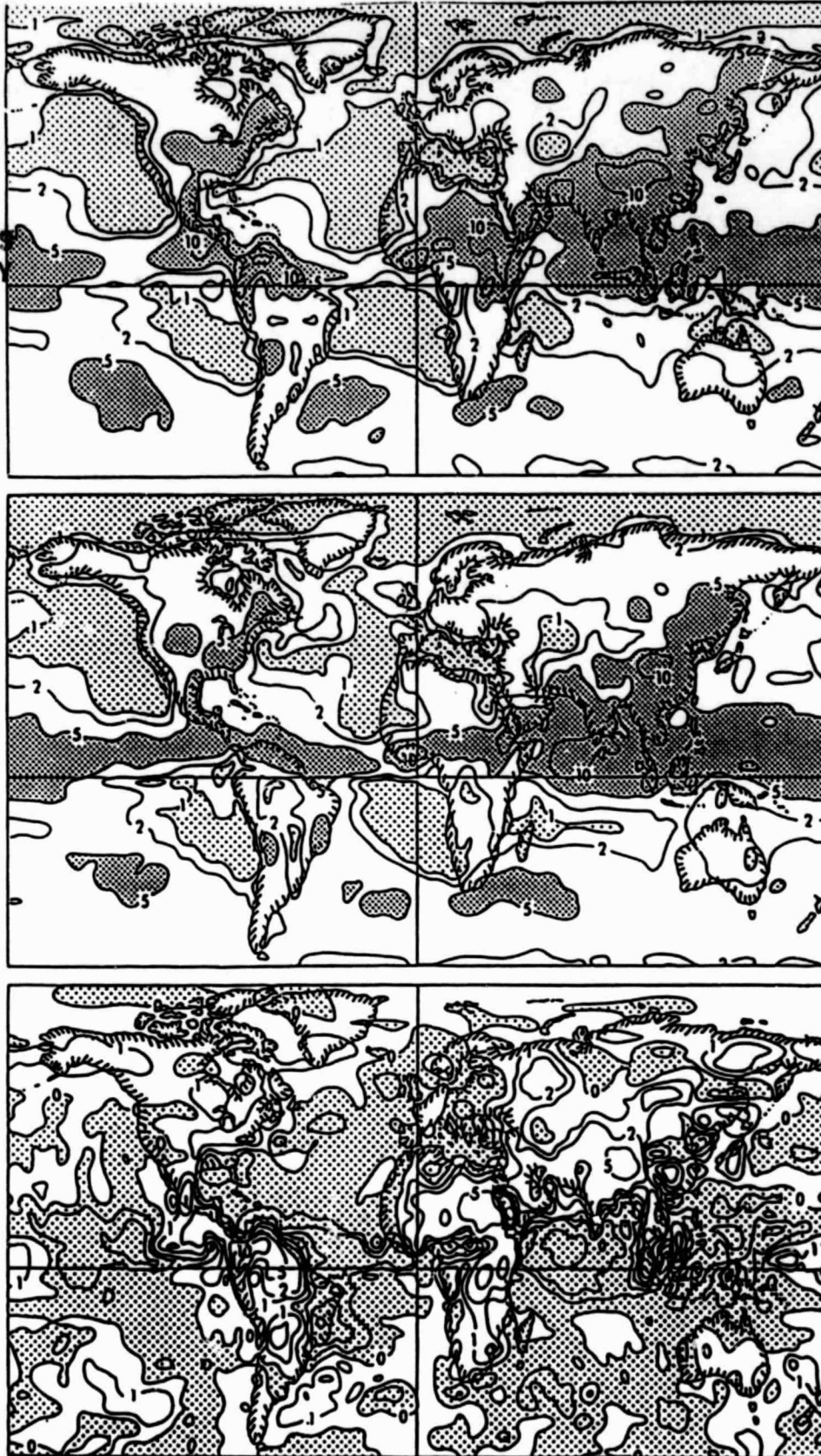
Fig. 12   Precipitation in the low albedo case (top) and the high
albedo case (center), of the experiment by Carson and Sangster (1981).
The contours are for 1, 2, 5, 10 and 20 mm/day. (Light shading, precip
< 1 mm/day; heavy shading, precip > 5 mm/day). The bottom panel
is the difference in the precipitation: the low albedo case minus the
high albedo case (unshaded area positive).

only about a third as large as is the contribution by the change in the local
evapotranspiration. Both experiments have about the same average water vapor
transport convergence, 0.8 mm/day vs. 0.85 mm/day. But in (4), where the albedo
was changed from 0.14 to 0.35 over a number of small regions, the average change
in the transport convergence in those regions was -1.2 mm/day. In (5), where
the albedo was changed from 0.1 to 0.3 over all of the land, the change in the
transport convergence was only -0.3 mm/day; showing, again, that the larger
the horizontal scale the smaller is the role of the water vapor transport con-
vergence in compensating for a decrease in the land-surface evapotranspiration.

Table II. Components of the energy and water budgets, in the experiment
of Carson and Sangster (1981)

Global Averages Over Land. 90-day means (Days 21-110) of a permanent July.

Sfc. Albedo	(1) LE	(2) H	(3) E	(4) $(-\overline{\nabla \cdot q \, \underline{v}})$	(5) P	(6) $\dfrac{\Delta(-\overline{\nabla \cdot q \, \underline{v}})}{\Delta E}$	(7) $\dfrac{\Delta P}{\Delta E}$
0.1	104	35	3.6	1.0	4.6		
0.3	78	21	2.7	0.7	3.4		
Difference	-26	-14	-0.9	-0.3	-1.2	0.3	1.3

For definition of symbols, see Table I.

II. EXPERIMENTS WITH INTERACTIVE SOIL MOISTURE

In all but one of the experiments that follow, the time-dependent soil moisture is governed by the equations:

$$\frac{\partial W}{\partial t} = P - E, \quad W_{max} = W^* \quad , \tag{1}$$

$$E = \beta \, E_p \quad , \tag{2}$$

$$\beta = \frac{W}{kW^*} \, , \quad \beta_{max} = 1 \quad , \tag{3}$$

where W is the available moisture stored in the soil, W* is the available moisture storage capacity of the soil, P is the rate of precipitation, E is the rate of evapotranspiration, E_p is the rate of potential evapotranspiration, β is the soil moisture availability, and k is a prescribed coefficient (cf. Carson, 1981). In all of the models, E_p is evaporation calculated by an aerodynamic method, under the assumption that the vapor pressure at the surface is the saturation value for the calculated ground temperature.

A. Different Initial Soil Moistures, with Same Albedo.

(6) Walker and Rowntree (1977).

Walker and Rowntree (1977) examined the interaction between time-dependent soil moisture and the calculated precipitation, temperature and circulation of the atmosphere, not in the global domain, but in a zonal channel between latitudes 16°S and 36°N, and extending over 32° of longitude with cyclic east-west boundary conditions. The land and sea distribution was made zonally-symmetric, with land to the north and ocean to the south of 6°N latitude; this being an idealization of the western part of north Africa and the Gulf of Guinea.

The model was an 11-layer primitive equations model with 2° latitude-longitude resolution. The radiational part of the thermal forcing was taken as a constant radiational cooling of the atmosphere, of 1.2°K per day from the surface to the 200 mb level, with radiative equilibrium at higher levels (which means a constant radiational cooling of the atmosphere of 110 watt/m^2); and with a constant net radiational heating of the land-surface, R_N, of 150 watt/m^2. Thus, over the land, there was a prescribed horizontally-uniform radiational heating (of 40 watt/m^2) of the atmosphere-earth system; but over the ocean, the surface temperature, and not the surface radiation flux, was the prescribed boundary condition. The prescribed, zonally-symmetric ocean temperatures, from 16°S to 6°N, were the observed August normals at 0° longitude. The moist-convective adjustment scheme was used to obtain the convective precipitation and moist-convective heating of the air.

The available soil moisture and the land-surface evapotranspiration were calculated with the equations given at the beginning of this section; with W* taken as 150 mm, and k taken as 0.333. Therefore, $\beta = 1$ when $W \geq 50$ mm.

Two integrations were made, in which everything was the same, except that:

In Case I (the initially dry-soil Sahara), W was initialized at zero in the latitude zone 14°N - 32°N; and at 100 mm in the land zones 6°N - 14°N and 32°N - 36°N.

In Case II (the initally moist-soil Sahara), W was initialized at 100 mm over all of the land region, 6°N - 36°N.

Fig. 13   Figures 13, 14 and 15 show the time-evolutions of the soil moisture and precipitation in the two cases.

In Case I (Fig. 13), where the soil was initially dry between 14° and 32°N, it remains dry. There is almost no net water vapor transport into that region and, therefore, there is no precipitation and no water is added to the soil there. On the other hand, in the land region 6°N - 14°N the initial soil moisture, of 100 mm, goes down to about 90 mm over the first seven days, showing an excess of evapotranspiration over precipitation which averages about 1.4 mm/day. The corresponding seven day water vapor transport divergence, of about 1.4 mm/day, is the difference between a large northward transport of water vapor across the coastline by the mean meridional circulation (Walker and Rowntree, 1977, Fig. 4.a) and an even larger equatorward eddy-transport of water vapor by the wave disturbance which developed and moved westward across the region. By the end of the integration period, this part of the system also appears to have reached a steady state, except for a short period and small amplitude variation produced by transient waves in the flow.

Figs. 14,15   In Case II, the initially moist-soil Sahara, (Figs. 14 and 15), there is a rapid development of precipitation in the zone near the coast which, after about 2 days, exceeds the evapotranspiration rate and the soil moisture

Precipitation (mm/day)
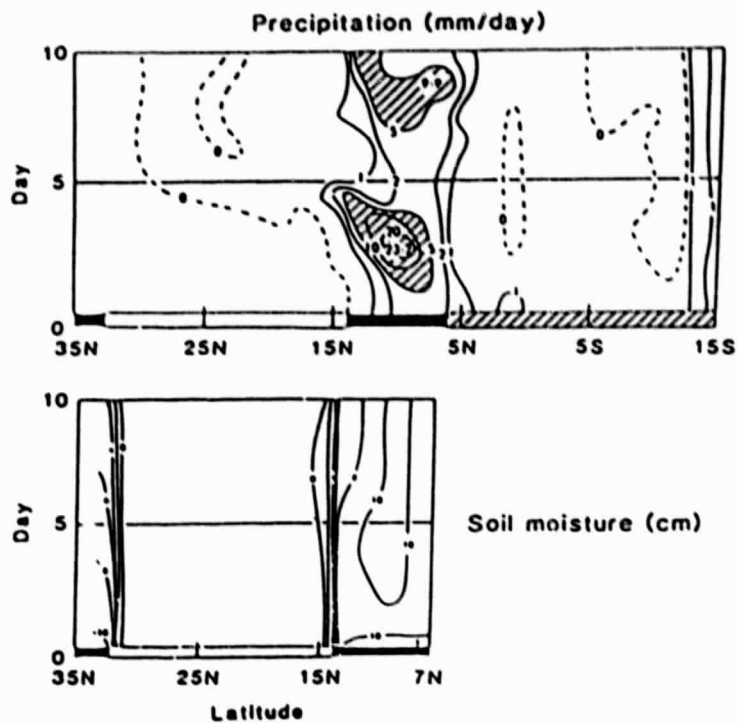

Soil moisture (cm)

Latitude

Fig. 13   Variation with time of the zonally-averaged precipitation (top) and soil moisture (bottom) in the case where initially the soil in the Sahara is completely dry.   Experiment of Walker and Rowntree (1977).
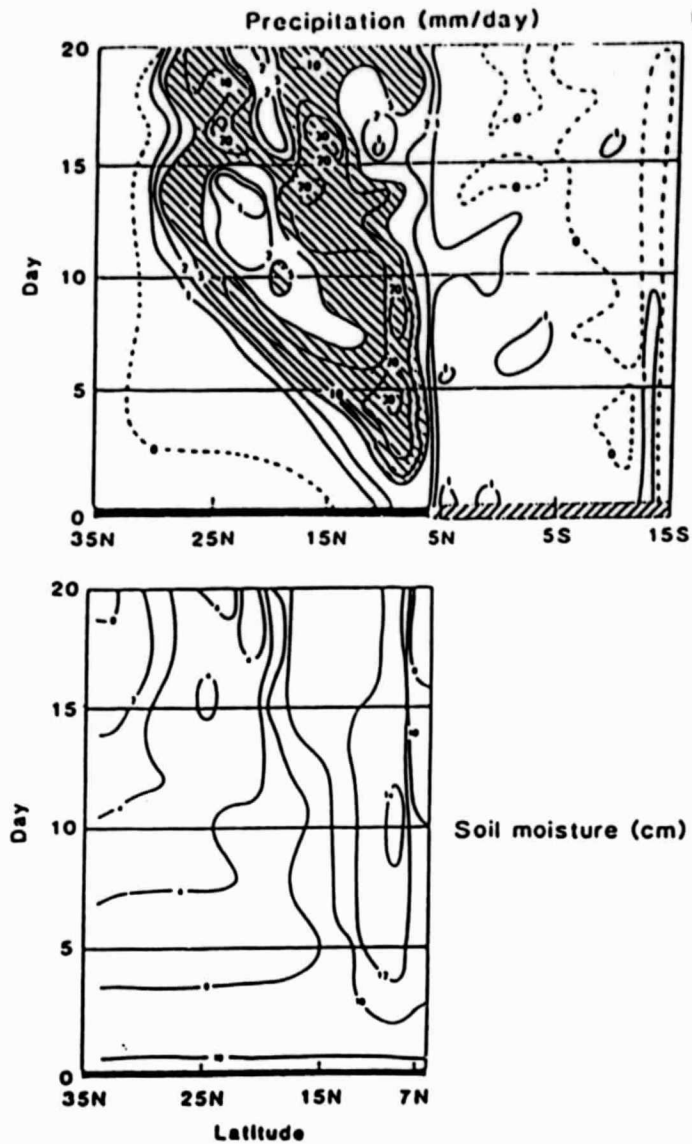
Fig. 14   Variation with time of the zonally-averaged precipitation
(top) and soil moisture (bottom) in the case where the initial soil mois-
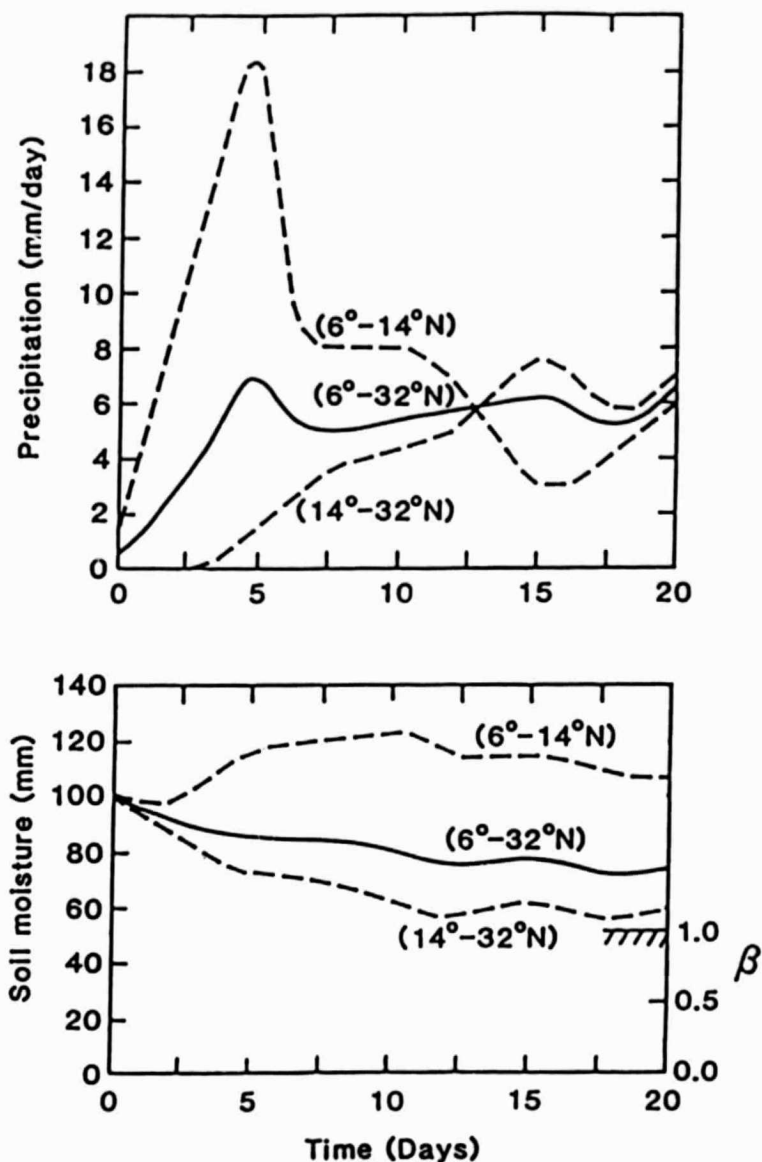ture in the Sahara is 100 mm.   Experiment of Walker and Rowntree (1977).

Fig. 15   Variation of the zonally-averaged precipitation and soil
moisture with time, in selected latitude zones across north Africa, in
the case where the initial soil moisture in the Sahara is 100 mm.
Experiment of Walker and Rowntree (1977).

starts to increase. The average precipitation in this coastal zone reaches 18 mm/day on day 5; with a maximum of 30 mm/day at 9°N. After that the precipitation rate in this zone decreases rapidly and seems to be starting an oscillation about an average rate of around 6 mm/day. The prescribed $R_N = 150$ watt/m^2 would provide enough energy for $E = E_p = 5.2$ mm/day; but the calculated evapotranspiration may be smaller or larger than this, depending on whether the sensible heat transfer at the surface is upward or downward.

Over the rest of the land region, 14° - 32°N, the evapotranspiration exceeds the precipitation until about day 12; and, thereafter, except for an oscillation produced by the transient wave disturbances, evapotranspiration equals precipitation and the soil moisture remains constant.

From what we see in these figures, it appears unlikely that the solutions for the initially dry-soil Sahara and the initially moist-soil Sahara will approach one another no matter how long the integrations were to continue. It seems safe to say that this highly simplified soil moisture-atmosphere system is intransitive.

(7) Rowntree and Bolton (1978).

Rowntree and Bolton (1978) made an interactive soil moisture experiment
with the 5-layer, 500 km grid size, version of the British Meteorological
Office general circulation model (described by Corby et al., 1977).

For the calculation of the soil moisture and evapotranspiration,
W* was taken as 200 mm and k as 0.5; so that $\beta = 1$ when $W \geq 100$ mm.

Three 50 day integrations were made, all starting from the same initial
atmospheric conditions on 27 May, but with different initial distributions of
soil moisture.

In one run, designated C (for control), the initial soil moisture was
set at 50 mm at all land points over the globe. Therefore, the initial soil
moisture availability, β, was 0.5 everywhere.

In the run designated W (for wet-soil case) the initial soil moisture
was set at 150 mm at all of the European land points that are within the re-
gion enclosed by the rectangle in Fig. 16; but with an initial value of 50 mm
at all other land points over the globe. Thus, the inital β was 1 in the
European region, but again 0.5 at all other landpoints over the globe.

In the run D (the dry-soil case) the soil moisture in the European
region was initialized at 0 mm (but, again, at 50 mm elsewhere). Now, the
initial β, and hence the initial evapotranspiration, was zero in the European
region.

Fig. 16

Fig. 17

Figure 16 shows maps of the three rainfall distributions, averaged for
the 30-day period 15 June - 15 July; and Fig. 17 shows meridional profiles of
those time-averaged rainfalls along longitude 13°E, where the maximum rainfall
occurs. In general the differences between the 30-day rainfalls are comparable
to what are produced by the natural variability of a model atmosphere with
fixed surface boundary conditions. But within the European region the time-
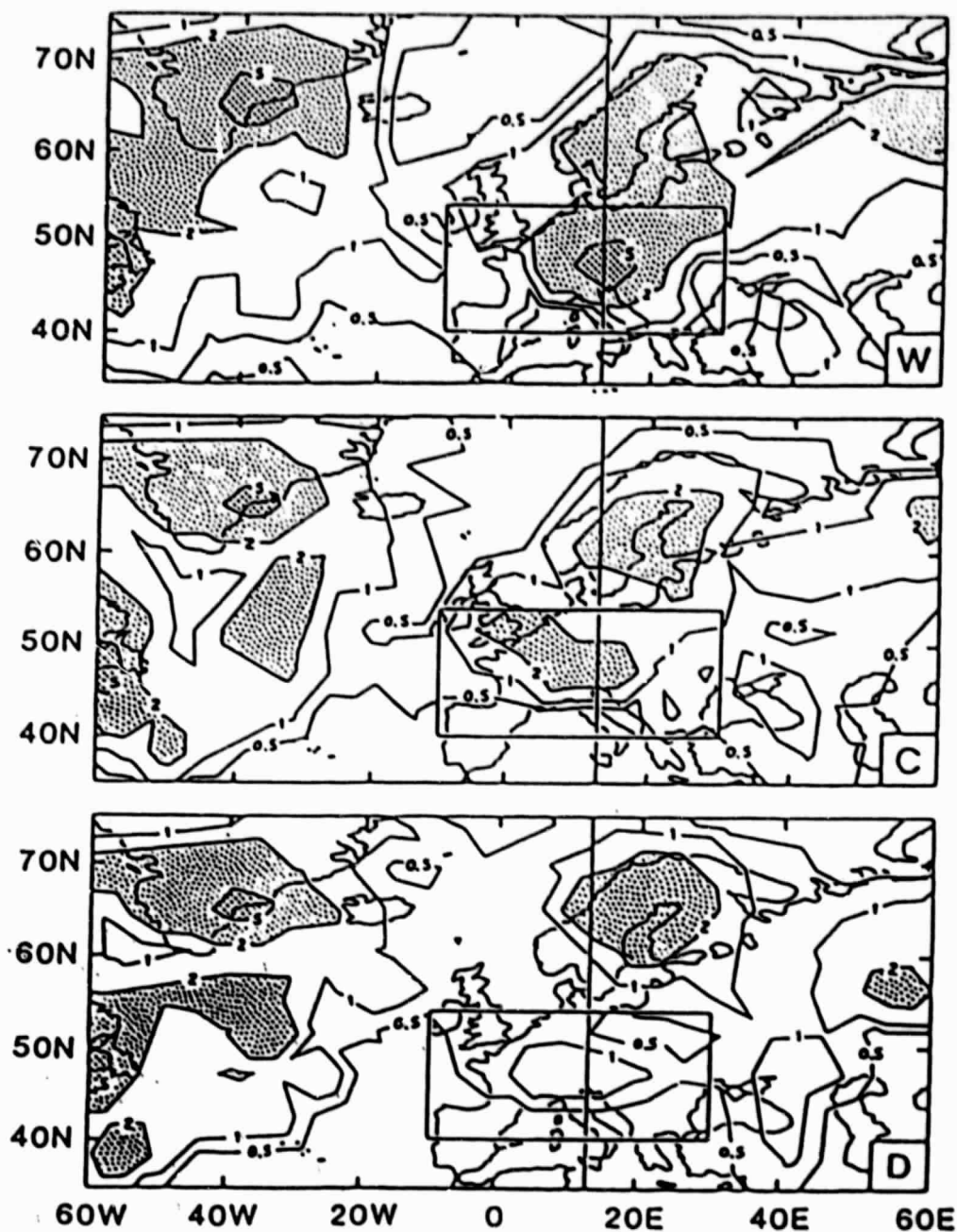
-32-

Fig. 16   Precipitation (mm/day) averaged for 15 June - 15 July, in
experiment of Rowntree and Bolton (1978).   Center panel: control run,
where the initial soil moisture, on 27 May, was 50 mm everywhere.   Top
panel: case where the European land points within the indicated
rectangular region had an initial soil moisture of 150 mm.   Bottom panel:
case where the European land points within the indicated rectangular
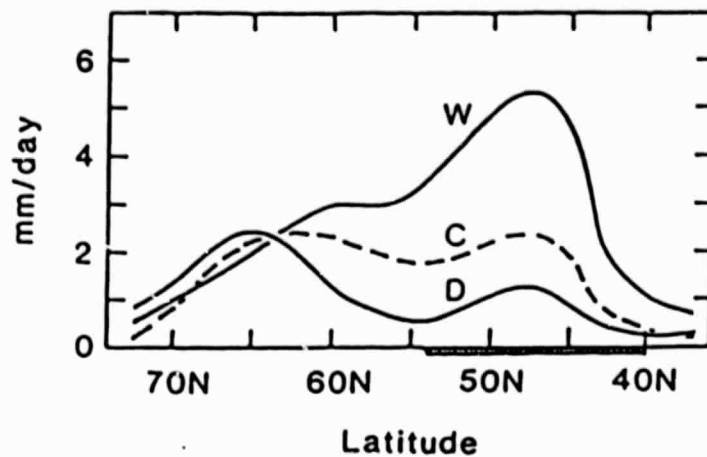region had zero soil moisture.

Fig. 17   Distribution of precipitation along the 13°E meridian, for the three fields shown in Fig. 16.

averaged precipitation, for days 20 to 50 following initialization, was greatest in the case which initially had the most moisture in the soil, and smallest when the soil was initially devoid of moisture.

The changes in the precipitation and in the soil moisture with time are shown in Fig. 18, where the values are 10 day averages for the indicated European land region. We see that even after one and a half months there are still large differences between the precipitation rates and between the soil moistures, when we compare the initially wet-soil case (W initially 100 mm) with the other two case (W initially 50 mm and 0 mm). The slopes of the rainfall curve and soil moisture curve, for the initially wet-soil case, suggest that the system is transitive; but that the time required for convergence is several months.
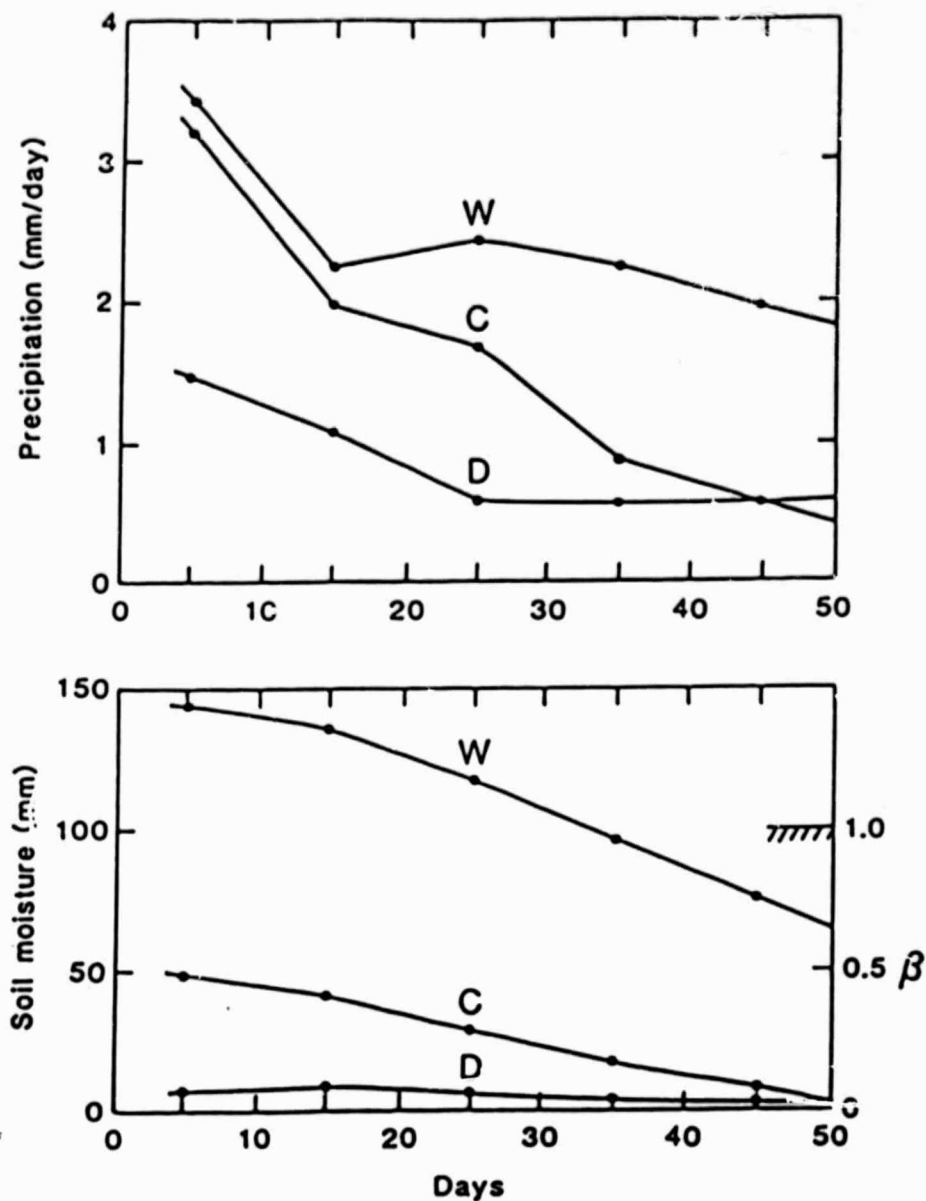
Fig. 18

-33-

Fig. 18 Variation with time of 10-day averaged precipitation (top) and soil moisture (bottom), averaged for the Euopean land points within the rectangular region shown in Fig. 16, for the three cases in the experiment of Rowntree and Bolton (1978).

B. Different Albedos, with Same Initial Soil Moisture.

(8) Charney, Quirk, Chow and Kornfield (1977).

Charney et al. (1977) made an experiment in which they compared two runs
which had different time-constant albedo distributions, but the same initial
soil moistures which could interact with the atmosphere.

The distribution of the land-surface albedo in the two cases is shown in
the bottom panel of Fig. 19. In their run designated "2b", the albedos of
"permanent desert" (the regions with dotted shading) were assigned the value of
0.35; and everywhere else over the ice-free and snow-free land surface of the
globe the albedo was taken as 0.14. In the comparison run, designated "3b",
three regions adjacent to the permanent deserts, the "Western Great Plains",
"Rajputana" and "Sahel" (shown by the cross-ruled shading) were also assigned
an albedo of 0.35. In both runs, the initial soil moisture was taken to
be zero everywhere.

The change in the time-dependent soil moisture was calculated, in half-
hourly time steps, from Eqs. (1) and (2) given at the beginning of this section,
and with the function $\beta = \beta$ (W, W^*, E_p) (Charney et al., 1977, p. 1368) which is
shown in Fig. 20. (Figure by personal communication from Y. Sud.) Over the
range of E_p between 1.4 and 6.4 mm/day, this formulation for β was taken from
Denmead and Shaw (1962), who obtained it from measurements of daily (24 hr)
evapotranspiration and potential evapotranspiration, together with measured
soil moisture.

In the experiment, this formula for β was inadvertently applied to the
calculation of half-hourly values of evapotranspiration, and this made the
calculated daily evapotranspiration an order of magnitude too small (because
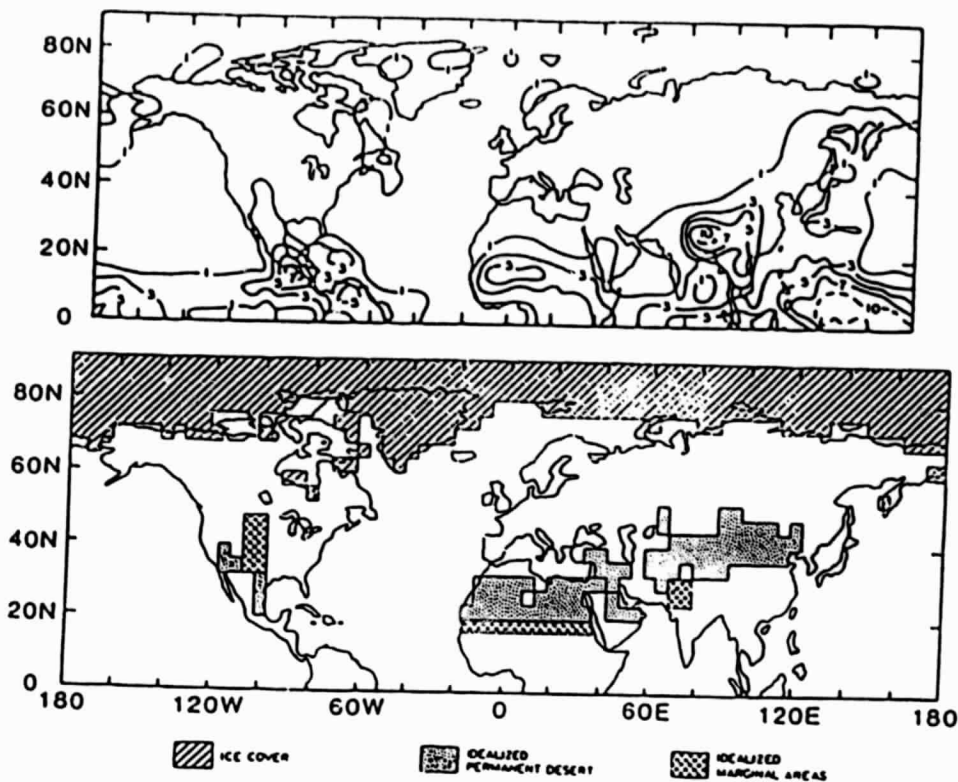during the mid-day hours, when E_p is about π times as large as its 24 hour

-34-

Fig. 19   Bottom panel: the assigned albedos in the experiments
of Charney et al. (1977).   Unshaded land areas have an albedo of 0.14 in
all cases, and dot-shaded areas have an albedo of 0.35 in all cases.   In
the cross-ruled areas the albedo was changed from 0.14 (in cases 2a and
2b) to 0.35 (in cases 3a and 3b).
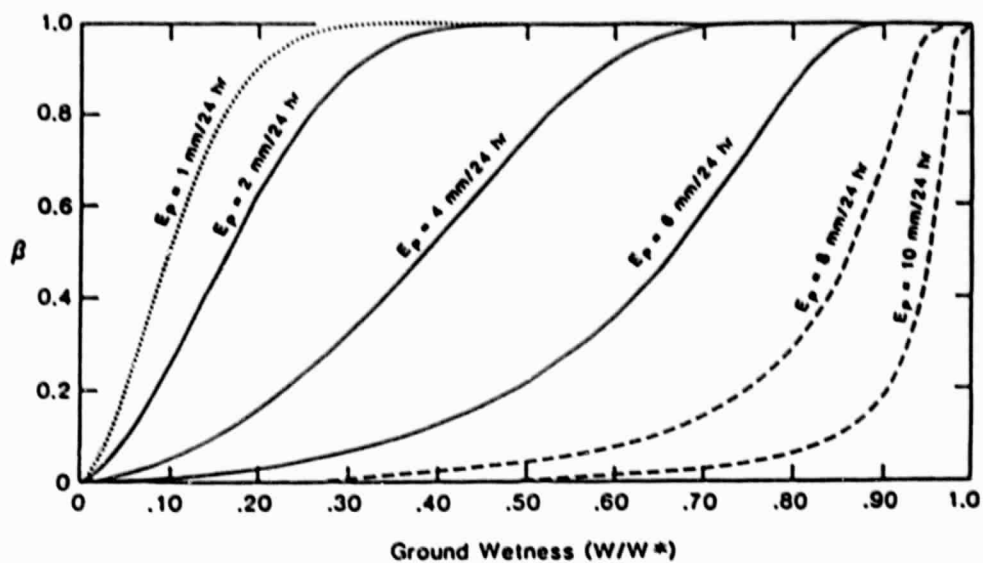   Top panel, precipitation (mm/day) in case 3b.

Fig. 20 The soil moisture availability function, $\beta = \beta(W, W^*, E_p)$, used by Charney et al. (1977) in the albedo experiment with interactive soil moisture.

average, the β obtained in this way is extremely small for almost all values

of W/W*; and during the night, when β can approach 1, E_p is negligible).

The top panel in Fig. 19 shows the calculated July precipitation in

Case 3b. At the beginning of the run, 18 June, almost all of the precipita-

tion that falls on the land must be from water vapor transported from the

ocean; and this situation must continue (because evapotranspiration is

negligible) until the accumulation of the water in the soil brings W close

to the soil storage capacity W*, at which point β becomes equal to 1 for

all values of E_p. For a precipitation of 5 mm/day, which is the mean

July precipitation across north Africa in Case 3b, it takes about 20 days,

or until about 8 July, for the soil moisture, W, to approach or reach W*,

at which point β approaches or reaches 1. Elsewhere, β remains negligible

until even the end of July. It is therefore not surprising that in this

experiment with interactive soil moisture the precipitation, for days 14-44

following initialization with zero soil moisture, should resemble the per-

sistently dry soil case shown in the lower panel of Fig. 3.

Table III   Table III shows the energy and water balances of the three regions, in

the two runs, for July (days 14 to 44 of the integration). We see, by

comparing columns (11) and (12), that during this period (which, as indicated,

is a transient stage for the soil moisture and evapotranspiration) the domin-

ant term in the supply of water vapor for precipitation, in all cases, is

the water vapor transport convergence. In the Sahel, the evapotranspirations

for the month are   0.14 and 0.34 mm/day, which are only 4% and 12% of the

monthly averaged precipitation rates. But almost all of this must be due

to the evapotranspiration near the end of July, at which time, or shortly

thereafter, the accumulated precipitation will make W approach or equal W*.

With the small amounts of evapotranspiration, the cloud cover (column 8)

Table III. Components of the energy and water budgets, in experiment of Charney et al. (1977)

Region	Case No.	(2) $(1-\alpha)$	(3) R_S	(4) R_L	(5) R_N	(6) LE	(7) H	(8) N	(9) T_A	(10) E	(11) $-qv$	(12)
					Energy Balance						Water Balance	
Sahel	2b	0.86	259	139	120	4	116	40	39.2	0.14	3.9	4.0
	3b	0.65	213	140	73	10	63	35	36.1	0.34	2.4	2.7
		-24%	-46	1	-47	6	-53	-12%	-3.1	0.20	-1.5	-1.3
Rajputana	2b	0.86	269	134	135	3	132	43	35.1	0.10	2.0	2.1
	3b	0.65	219	129	90	8	72	42	34.2	0.26	2.1	2.4
		-24%	-50	-5	-45	5	-60	-2%	-0.9	0.16	0.1	0.3
Western Great Plains	2b	0.86	302	172	130	0	130	21	37.5	0.00	0.8	0.8
	3b	0.65	245	161	84	3	81	20	31.4	0.10	0.3	0.4
		-24%	-57	11	-46	3	-49	-5%	-6.1	0.10	-0.5	-0.4

For definition of symbols, see Table I.

is not very different in the low and high albedo cases. Consequently, unlike Experiment (4) above, the change in the net radiational heating of the ground, R_N, is almost entirely due to the change in the solar radiational heating of the ground, R_S; and this produces the large change in the sensible heat transfer, H. It is this change in the sensible heating of the planetary boundary layer which produces the change in the vertical velocity shown in the bottom panel of Fig. 21; the associated change in water vapor transport convergence, shown in column (11) of Table II; and, the change in precipitation shown in column (12) and in the top panel of Fig. 21. As the experiment stands, it does illustrate the mechanism of the Charney (1975) "dry-soil" desertification hypothesis: but not if the integrations were to continue; for then W will everywhere approach or equal W* and the processes which depend on evapotranspiration will become important.

Fig. 21

We note, furthermore, that this simple picture of the coupling of the water vapor transport convergence to the surface albedo does not hold for the Rajputana and Western Great Plains regions, even when the evapotranspiration is negligibly small. In both of these regions the changes in R_S, R_N, and H are about the same as the changes in the Sahel; but, unlike the Sahel, there is almost no change in the water vapor transport convergence. As already indicated, the response of the atmospheric circulation to a change in the boundary layer heating, H, will depend very much on the horizontal scale and latitude of the heating perturbation, as well as on the orientation of the region with respect to external moisture sources and the way in which the altered flow encounters the mountain barriers.
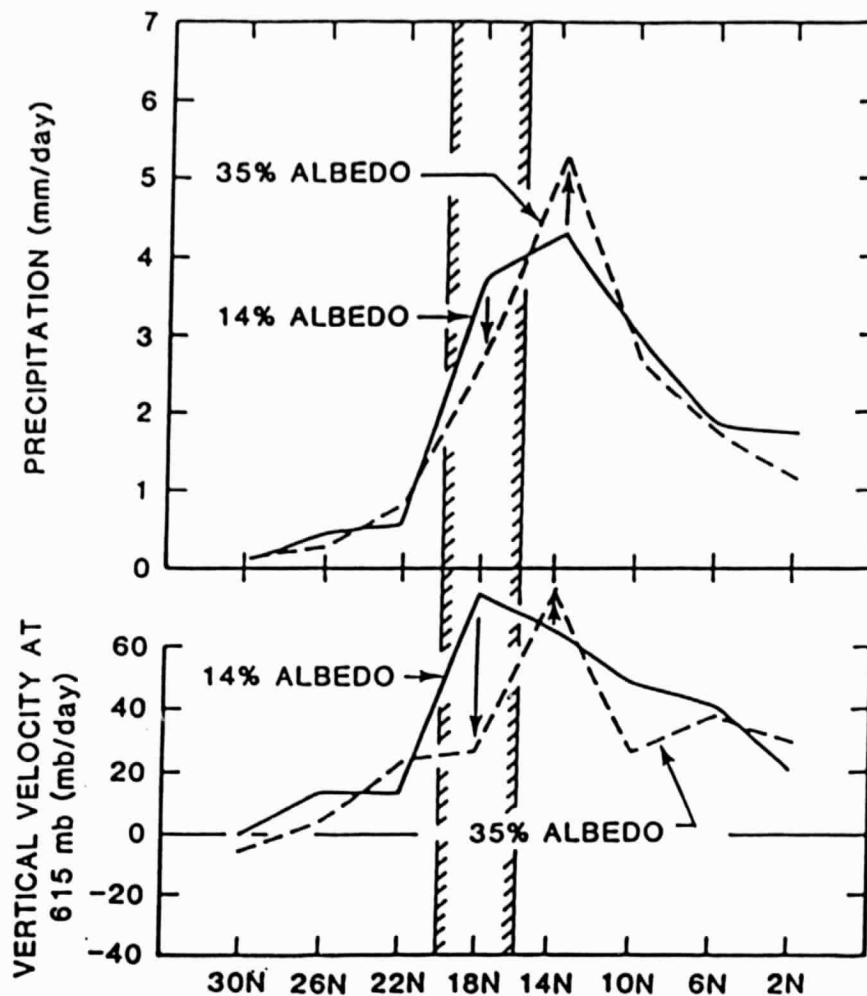
Fig. 21 Zonally-averaged precipitation (top) and vertical velocity in the middle troposphere (bottom), over Africa, when the albedo in the Sahel (16°N - 20°N) is increased from 0.14 to 0.35. Experiment of Charney et al. (1977).

(9) <u>Chervin (1979)</u>.

Chervin (1979) used the NCAR general circulation model (described by Washington and Williamson, 1977) to examine the effect of a change in the land-surface albedo when the soil moisture is fully interactive. The change in soil moisture was calculated with the equations given at the beginning of this section, with $W^* = 150$ mm and $k = 0.75$.

The control was the average of a master run, which started from a state of rest and isothermalcy and was integrated for 120 days, plus four other runs, each of which started from day 30 of the master and ran until day 120. All of these were perpetual July integrations, in which the sun declination, the ocean surface temperatures, and the snow-free land albedo (which followed Posey and Clapp, 1964) were held constant in time.

The run with a different albedo was also started from day 30 of the master and ran until day 120. The change in the albedo consisted of replacing the Posey and Clapp values by a constant albedo of 0.45 within two regions: 1) a large region over north Africa, extending from the Atlantic to the Red Sea and from latitude 7.5°N to the Mediterranean; and therefore covering the zone of the July intertropical convergence rain as well as the Sahara Desert; and 2) a smaller region over the U. S. High Plains (97.5°W - 107.5°W, 27.5°N - 52.5°N).
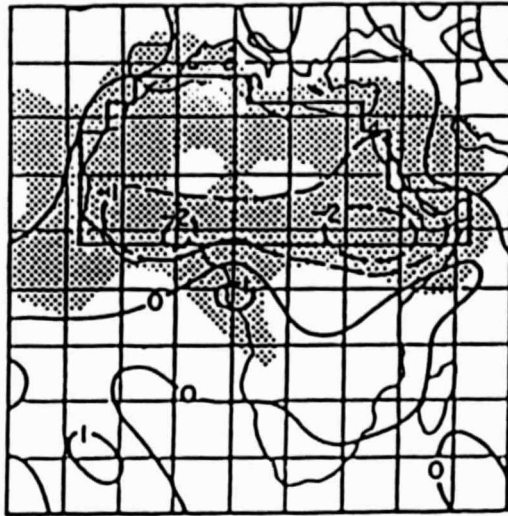
Over Africa, the control (Posey and Clapp) albedo varies from about 0.35 in the northern Sahara to about 0.08 near the southern boundary of the region where the albedo will be changed. Over the U. S. High Plains, the control albedo is between 0.07 and 0.17.
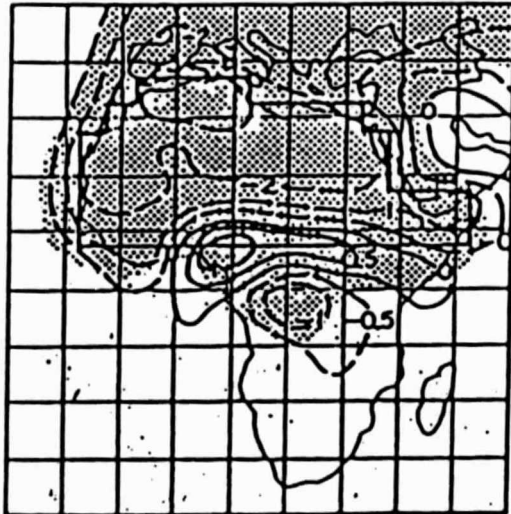
Fig. 22   Fig. 22 shows the change over Africa in the precipitation, soil moisture and ground temperature, and in the vertical velocity at 3 km elevation. The values shown are the averages of the last 60 days of the modified albedo case,

-38-

Δ 3KM VERTICAL VELOCITY (MM/SEC)   Δ PRECIPITATION RATE (MM/DAY)

Δ GROUND TEMPERATURE (°C)   Δ SOIL MOISTURE (CM)

Fig. 22 . The change in vertical velocity at 3 km elevation (top left), precipitation (top right), ground temperature (bottom left), and soil moisture (bottom right), in the albedo change experiment of Chervin (1979).

minus the ensemble average of the last 60 days of the five control runs. The stippled areas in the figure show the regions of $r = |\Delta_{60}|/\sigma_{60} \geq 3$; where Δ_{60} is the prescribed change response (i.e., the difference between the 60-day mean in the prescribed change case and the ensemble average of the 60-day means of the five control runs); and σ_{60} is the standard deviation of the 60-day means of the five control runs. According to Chervin and Schneider (1976), $r \geq 3$ implies an approximately 5% significance level in rejecting the hypothesis that the prescribed change response is the result of random fluctuations and not the result of the prescribed surface albedo change.

The maps in Fig. 21 show that the changes are greatest at and near the zone where the albedo is increased from 0.08 to 0.45. In this zone there is a decrease in the average upward motion of the air of about 2 mm/sec (200 m/day), with $r > 3$; a decrease in the average precipitation of about 4 mm/day, with $r \geq 2$, $[\Delta_{60} P = (4 - 8)$ mm/day, $\sigma_{60} P = 2$ mm/day]; and a decrease in the average soil moisture storage of about 50 mm, with $r > 3$. There is a decrease of the ground surface temperature, with $r > 3$, over almost all of the region of the albedo change, but not along its southern edge. There, the ground surface temperature increases, by about 0.5°C, with $r > 3$.

The paradoxical rise in the ground surface temperature, in the region of the largest increase of albedo (the change from 0.08 to 0.45), can be attributed to the fact that in that zone, 7.5°N - 12.5°N, where there is the largest decrease in precipitation, the soil moisture, W, goes down from about 100 mm in the control to 50 mm in the high albedo case. With $W* = 150$ mm and $k = 0.75$, this reduces β from 0.9 to 0.45, and, consequently, there is a large reduction in the evapotranspiration and the evaporative cooling of the surface in that zone. There is also a contribution to the temperature rise from the accompanying

reduction of the cloudiness in that zone (R. Chervin, personal communication).

Over the U. S. Great Plain region there was almost no change in the vertical velocity at 3 km elevation; an average decrease of about 1 mm/day in the precipitation, with $r > 3$ over about half of the region; almost no change in the soil moisture storage; and a decrease, averaging about 2°C, with $r > 3$, in the ground surface temperature.

Non-Interactive vs. Interactive Soil Moisture

These are experiments in which a calculation with interactive soil moisture is compared with one in which the prescribed soil moisture is held fixed for the duration of the experiment. If we regard the interactive case as a simulation of nature, then the case with the prescribed, fixed soil moisture can be thought of as showing how the climate would be changed if the land-surface evapotranspiration were to be brought under man's control: as, for example, by large scale irrigation or by a change or a complete removal of the vegetation cover.

(10) Manabe (1975)

A massive irrigation simulation experiment was made by Manabe (1975) with one of the GFDL general circulation models. The model used the moist-convective adjustment method for calculating the convective precipitation and the moist-convective heating of the air; solar and long wave radiation transfers calculated with a non-interactive cloud distribution, prescribed as a function of latitude and elevation; and an albedo for ice-free and snow-free land that follows Posey and Clapp (1964).

In the "natural-case" (the interactive soil moisture case) the soil moisture was governed by the equations given at the beginning of Section II, with $W* = 150$ mm, and $k = 0.75$. In the "irrigation-case" (the non-interactive soil moisture case) β was everywhere held equal to 1.

The "natural-case" simulation produced a rainband across north Africa in in which, averaged between 15°E and 30°E, there was a rainfall maximum of about 6 mm/day at latitude 5°N. In the irrigation-case, the maximum rainfall was about 12 mm/day at latitude 8°N (see Manabe, 1975, Fig. 3).

Fig. 23   The solid line in Fig. 23 shows the change in the precipitation, the
irrigation-case minus the natural-case. The dashed line shows the corresponding
difference in the evapotranspiration. (The reduction in evaporation, between
31°N and 37°N, is over the Mediterranean Sea; presumably because the air was
more humid from the massive land irrigation).

Between 18°N and 30°N the increase in precipitation is somewhat less than
the increase in evapotranspiration, while between 12°N and 15°N, where the
evapotranspiration increases by only about 1.5 mm/day, the precipitation goes
up by about 5.5 mm/day. On the other hand, at the equator, where there is an
increase of evapotranspiration of 0.7 mm/day, the precipitation decreases by
3.5 mm/day. It is obvious, therefore, that there are large changes in the
water vapor transport convergence.

Fig. 24   Figure 24 shows the circulation in the meridional plane, $(v\,\mathbf{j} + w\,\mathbf{k})$,
averaged between 15°E and 30°E (where v is the northward component of the
horizontal velocity, w is the vertical velocity, $\mathbf{j}$ is unit horizontal vector
directed northward, and $\mathbf{k}$ is unit vertical vector directed upward). Although
the eastward component of the horizontal velocity does not appear here, its
divergence, $\partial u/\partial x$, enters into the calculation of the vertical velocity, w.

We see that at the equator there is a change from upward motion to down-
ward motion in the free atmosphere; which must be accompanied by a change
from horizontal velocity convergence to horizontal velocity divergence in
the boundary layer. It therefore is the decrease in the boundary layer water
vapor transport convergence $(-\overline{\nabla \cdot q\,\mathbf{v}} = -\overline{q\nabla \cdot \mathbf{v}})$ which makes the precipitation
decrease by 3.5 mm/day (from 5 to 1.5 mm/day).

Between 12°N and 15°N, on the other hand, weak ascending motion changes
to very strong ascending motion; and the accompanying large increase in the
boundary layer water vapor transport convergence, added to the small increase
in evapotranspiration, makes the precipitation increase by 5.5 mm/day (from
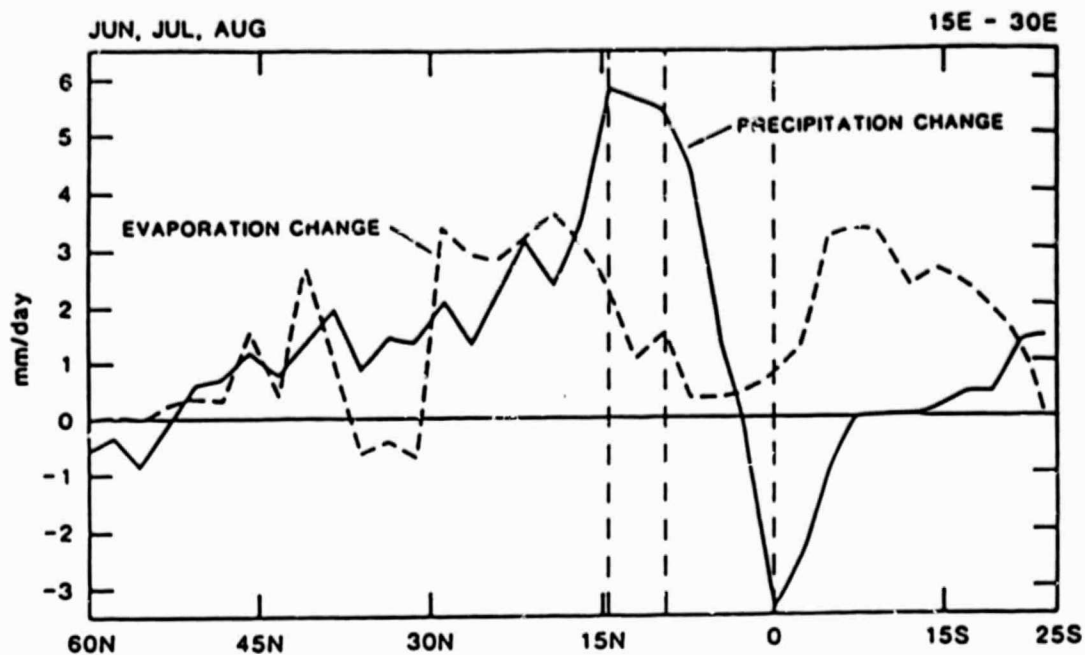0.7 to 6.2 mm/day).

Fig. 23 Change in evapotranspiration (broken line) and in precipitation (solid line), averaged between 15°E and 30°E, in the hybrid experiment of Manabe (1975).
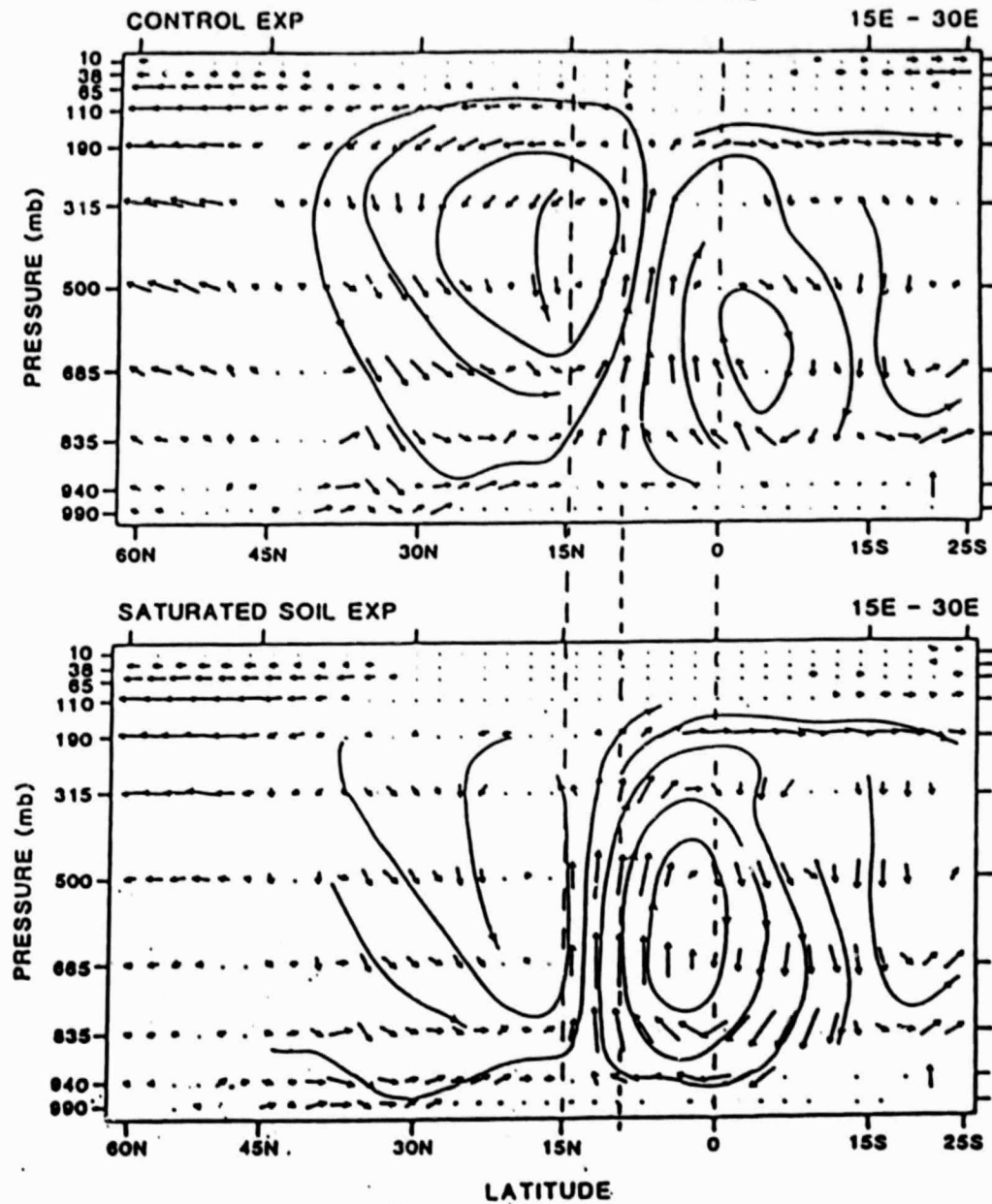
Fig. 24   Circulation in the meridional plane, averaged between 15°E and 30°E, in the hybrid experiment of Manabe (1975).   Top: interactive soil moisture case.   Bottom: moist soil case.   (figure by personal communication)

(11) Kurbatkin, Manabe and Hahn (1979).

The irrigation scheme of Experiment (10) (which makes β = 1 everywhere)
is physically realizable in the real world. But it is not so easy to make
β = 0 everywhere in the real world. If the rainfall were to be very constant
in time, so that the surface of the earth was always wet, then it would be
very difficult (although possible) to prevent evaporation. But where rainfall
occurs in an intermittent way, and most of the water infiltrates to a depth of
more than a few centimeters, then the removal of the vegetation would stop the
transpiration and, thereby, would greatly reduce the transfer of water vapor
to the air.

Kurbatkin, Manabe and Hahn (1979) made a hybrid experiment, in which a
simulation with β = 0 everywhere was compared with a simulation with inter-
active soil moisture. For this experiment they used the M-21 version of the
GFDL spectral model (Manabe, et al., 1979), with moist-convective adjustment,
prognostic clouds, and a prescribed albedo that follows Posey and Clapp (1964).
In the interactive soil moisture case, the soil moisture and evapotranspira-
tion were calculated with the equations given at the beginning of Section II,
with W* = 150 mm, and k = 0.75.

The integration in the interactive case was over a period of two years
and eight months. The results that are shown here are averages for the months
of July and August at the end of the integration period. The non-interactive
case, with β = 0, was initialized from the interactive case at the beginning
of the last June and run until the end of August.

Fig. 25   The top panel in Fig. 25 shows the simulated precipitation in the
interactive soil moisture case, the center panel shows the precipitation
in the no-evapotranspiration case, and the bottom panel shows the difference
between the two (no-evapotranspiration case minus interactive case). With
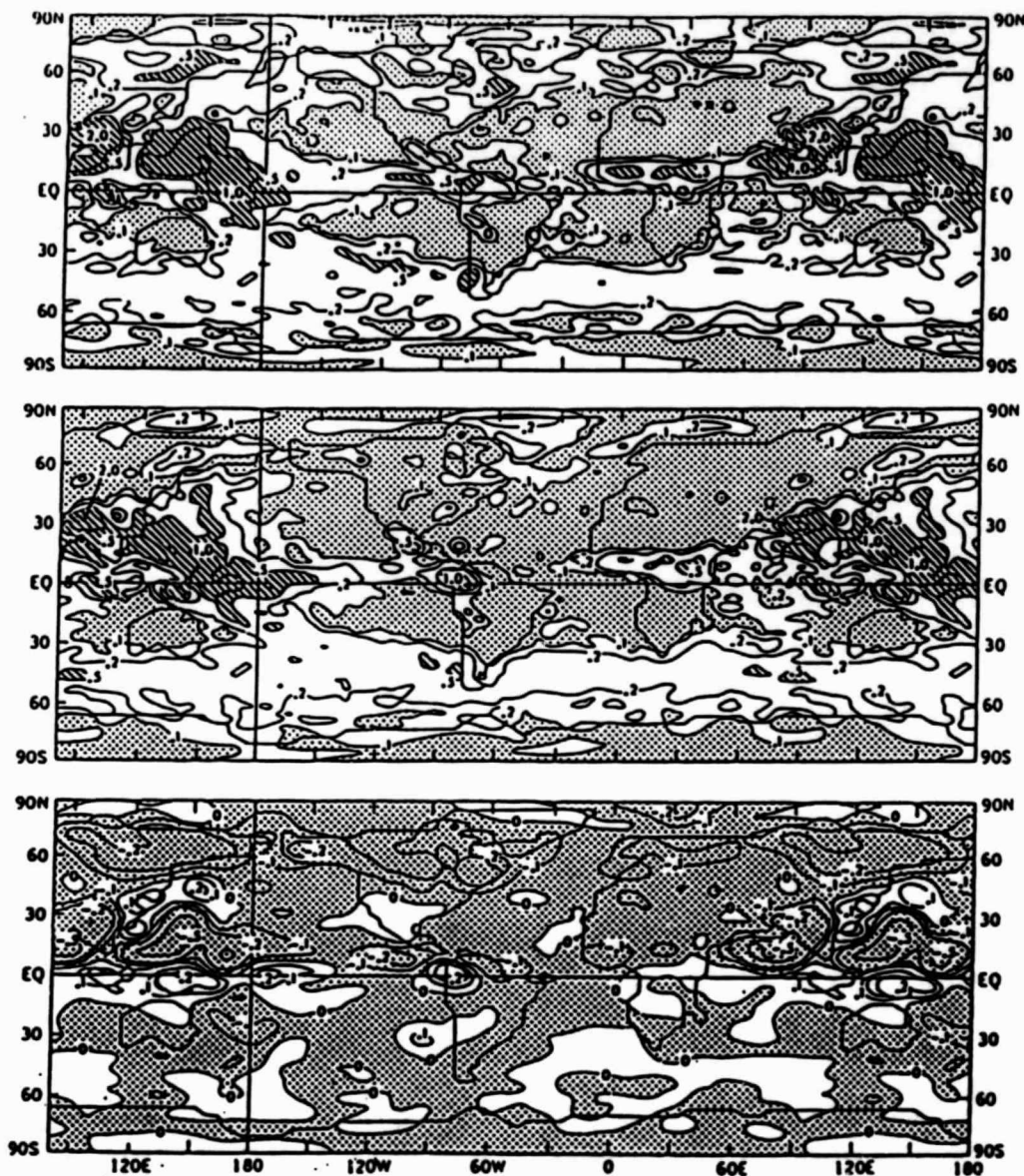
-43-

Fig. 25   Precipitation (cm/day) averaged for July and August, in the experiment of Kurbatkin et al. (1979). Top: interactive soil moisture case. Middle: no land-surface evapotranspiration case. (Contours 0.05, 0.1, 0.2, 0.5, 1.0, 5.0 cm/day. Dotted shading: precip. < 0.1 cm/day; ruled shading: precip. > 0.5 cm/day).. Bottom: no-evapotranspiration case minus interactive case (shaded area negative).

no land-surface evapotranspiration, there is less precipitation over the
continents and also less precipitation over most of the oceans; with the largest
decreases, of up to 5 mm/day, over India, the north Indian Ocean and over the
western part of the tropical North Pacific. Only over the mid-latitude east
coast of Asia and the adjacent Pacific, and in some longitudes along the equator
(but not over the Atlantic Ocean sector), is the precipitation larger in the
$\beta = 0$ case, and by as much as 2 mm/day.

Fig. 26   Fig. 26 shows the sea level pressure fields. We see that in the no-
evapotranspiration case the pressure is lower over most of the continental
areas. But over north-central Asia, over the northeast Atlantic, and espe-
cially over the extratropical central and western North and South Pacific
Oceans, the pressures are higher in the no-evapotranspiration case. Although
only the $\beta = 0$ case has the same evapotranspiration boundary condition that
was used in the experiment with the GLAS model (Experiment 1 above), there
are many correspondences, as can be seen by comparing the bottom panels
Fig. 25 and Fig. 6, especially over the central and western North and South
Pacific and over the South Atlantic.

The authors show (Kurbatkin et al., 1979, Fig. 4) that in the $\beta = 0$
case there is, on the average, an increase in the large scale ascending motion
in the free atmosphere over the continents; and they remark that in spite of
this increased ascending motion there is less cloudiness over the continents;
and therefore a greater absorption of solar radiation by the ground and a
higher surface temperature than in the interactive soil moisture case. The
decrease in the precipitation over the oceans, they point out, is produced
by the increase in descending motion (or weakening of ascending motion) over
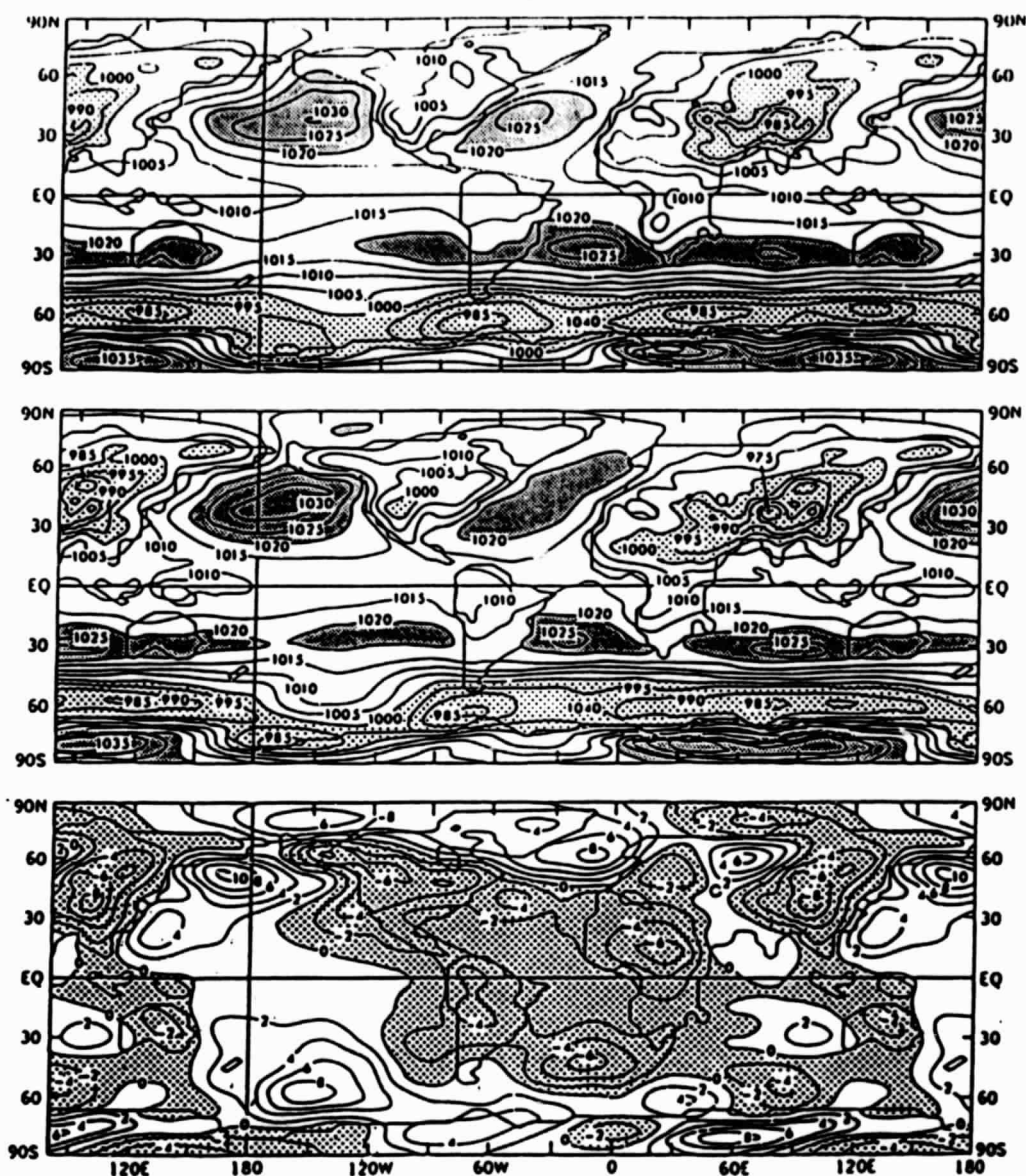the oceans.

Fig. 26   Sea level pressure (mb), averaged for July and August, in
the experiment of Kurbatkin et al. (1979).   Top: interactive soil moisture
case.   Middle: no land-surface evapotranspiration case.   Bottom: no-
evapotranspiration case minus interactive case (shaded area negative).

All of the experiments show that the model simulated climates are sensitive to the land-surface boundary conditions which affect evapotranspiration. When soil moisture availability or surface albedo are changed regionally (or globally), changes in the precipitation, the temperature and the motion field of the atmosphere take place over the corresponding region (or over the globe), which are clearly above the level of the natural variability of the model simulated climates (those which are caused by the shear-flow instabilities of the atmosphere).

[Whether a change in the boundary condition of a given region has a significant effect on the climate of some distant region is not known. Such atmospheric "teleconnections" are not self-evident in these experiments: and, like other kinds of forcing from a distance, they require some kind of statistical analysis to separate the signal from the background noise].

Not only are the regional (local) influences large and consistent from one experiment to another; they are also easily understood, in physical terms, after the analysis has untangled the non-linear interactions. Thus we find, for example, that under some circumstances an increase in the surface albedo reduces the cloudiness and, in that way, increases (not decreases) the ground temperature. Or, as another example, cutting off the evapotranspiration over Asia increases (not decreases) the Indian monsoon rainfall, because it changes the orientation, with respect to the Himalayan mountain barrier, of the moist boundary layer air stream from the ocean. It is this kind of behavior, easily understood after the fact, which is very difficult to anticipate beforehand.

The magnitudes of the changes in climate which are produced by modifying the soil moisture availability or the surface albedo, as shown in these experiments, are about as large as the changes produced by the seasonal change in

the declination of the sun (and, the reviewer hazards the guess, larger than the changes produced by the observed seasonal changes in ocean surface temperatures and extent of the sea-ice). It is very likely, therefore, that the land-surface evapotranspiration process, whose time scale depends on the magnitude of the soil moisture storage relative to the difference between the precipitation and evapotranspiration rates, is the most important boundary process that can produce anomalies in the time-averaged state of the atmosphere (changes in climate) on the monthly, seasonal and annual time scales.

A shortcoming of all existing general circulation models is that they calculate the potential evapotranspiration with a formulation which is appropriate for evaporation from an open water bucket, but not from a vegetated surface (and, especially, not from tall (forest) vegetation.) (See, for example, Shuttleworth and Calder, 1979; and Sellers and Lockwood, 1981). But, hopefully, this will be corrected and future models will take into account the vegetation influence on the water and energy transfers to the atmosphere in a realistic way.

.   .   .   .

ORIGINAL PAGE IS
OF POOR QUALITY

· · · · · · · · · · · · · · ·

Since this review was written four additional papers have appeared, all of which show that the atmosphere is sensitive to the land surface evapotranspiration.

Rind, D., 1982: The influence of ground moisture conditions in North America on summer climate as modeled in the GISS GCM. Mon. Wea. Rev., 110, pp. 1487-1494.

Rowntree, P. R. and J. A. Bolton, 1983: Effects of soil moisture anomalies over Europe in summer. Quart. J. R. Met. Soc. (in press)

Sud, Y. C. and M. Fennessy, 1982: A study of the influence of surface albedo on July circulation in semi-arid regions using the GLAS GCM. Journ. Climatology, 2, pp. 105-125.

Yeh, T. C., R. T. Wetherald and S. Manabe, 1983: The effect of soil moisture on the short-term climate and hydrology change - a numerical experiment. Mon. Wea. Rev. (in press)

REFERENCES

Arakawa, A. and V. R. Lamb. 1977: Computational design of the basic dynamical processes of the UCLA general circulation model. Methods in Computational Physics, 17 , pp. 173-265, Academic Press, N.Y.

Arakawa, A. and M. J. Suarez, 1983: Vertical differencing of the primitive equations in sigma coordinates. Mon. Wea. Rev. (in press)

Baumgartner, A. and E. Reichel, 1975: The World Water Balance: Mean Annual Global, Continental and Maritime Precipitation, Evaporation and Runoff. Elsevier Publishing Co., Amsterdam/Oxford/New York, 179 pp and plates.

Benton, G. S., M. A. Estoque and J. Dominitz, 1953: An Evaluation of the Water Vapor Balance of the North American Continent. The Johns Hopkins University Dept. Civil Engineering. Scientific Report No. 1, July 1953, 101 pp.

Budyko, M. I. (editor), 1963: Atlas of the Heat Balance of the Earth. With N. A. Efimova: Maps of the radiation balance for the continents. Plates 14-26.

Carson, D. J., 1981: Current Parameterization of Land Surface Processes in Atmospheric General Circulation Models. In Proceedings of the JSC Study Conference on Land-Surface Processes in Atmospheric General Circulation Models, Greenbelt, USA, 5-10 January 1981. WMO, Geneva.

Carson, D. J. and Sangster, A. B., 1981: The influence of land-surface albedo and soil moisture on general circulation model simulations. GARP/WCRP: Research Activities in Atmospheric and Oceanic Modelling. (Ed. I.D. Rutherford). Numerical Experimentation Programme, Report No. 2, pp. 5.14-5.21.

Charney, J. G., 1975: Dynamics of deserts and drought in the Sahel. Quart. J. R. Met. Soc., 101, pp. 193-202.

Charney, J. G., Quirk, W. J., Chow, S. H. and Kornfield, J., 1977: A comparative study of the effects of albedo change on drought in semi-arid regions. J. Atmos. Sci., 34, pp. 1366-1385.

Chervin, R. M., 1979: Response of the NCAR general circulation model to changed land surface albedo. Report of the JOC Study Conference on Climate Models: Performance, Intercomparison and Sensitivity Studies. Washington, D. C., 3-7 April, 1978. GARP Publ. Series, No. 22, Vol. 1, pp. 563-581.

Chervin, R. M. and S. H. Schneider, 1976: On determining the statistical significance of climate experiments with general circulation models. J. Atmos. Sci., 33, pp. 405-412.

Corby, G. A., Gilchrist, A. and Rowntree, P. R., 1977: The U.K. Meteorological Office 5-layer general circulation model. Methods in Computational Physics, 17, pp. 67-110.

Denmead, O. T. and R. H. Shaw, 1962: Availability of soil water to plants as affected by soil moisture content and meteorological conditions. Agron. J., 54, pp. 385-439.

Gadd, A. J. and J. F. Keers, 1970: Surface Exchanges of Sensible and Latent Heat in a 10-level Model Atmosphere. Quart. J. R. Met. Soc., 96, pp. 297-308.

Korzun, V. I. (ed), 1978: World Water Balance and Water Resources of Earth. Report of the USSR Committee for the International Hydrological Decade. Studies and Reports in Hydrology, vol. 25. Unesco Press, Paris, 663 pp and plates.

Kurbatkin, G. P., S. Manabe and D. G. Hahn, 1979: The moisture content of the continents and the intensity of summer monsoon circulation. Meteorologiya i Gidrologiya, 11, pp. 5-11.

Manabe, S., 1975: A study of the interaction between the hydrological cycle and climate using a mathematical model of the atmosphere. Proceedings of Conference on Weather and Food, Endicott House, Mass. Inst. Tech., Cambridge, Mass., 9-11 May 1975. 10 pp. (and additional figure by personal communication).

Manabe, S., D. G. Hahn and J. L. Holloway, Jr., 1979: Climate simulations with GFDL spectral models of the atmosphere: Effect of spectral truncation. Report of the JOC Study Conference on Climate Models: Performance, Intercomparison and Sensitivity Studies. Washington, D.C., 3-7 April 1978. GARP Publ. Ser., No. 22, Vol. 1, pp. 41-94.

Miyakoda, K., G. D. Hembree and R. F. Strickler, 1979: Cumulative results of extended forecast experiments II: Model performance for summer cases. Mon. Wea. Rev., 107, pp. 395-420.

Miyakoda, K., J. Smagorinsky, R. F. Strickler, and G. D. Hebree, 1969: Experimental extended predictions with a nine-level hemispheric model. Mon. Wea. Rev., 97, pp. 1-76.

Miyakoda, K. and R. F. Strickler, 1981: Cumulative results of extended forecast experiment. Part III: Precipitation. Mon. Wea. Rev., 109, pp. 830-842.

Posey, J. W. and P. F. Clapp, 1964: Global distribution of normal surface albedo. Geophisica Internacional, 4, No. 1, pp. 33-48.

Rasmusson, E. M., 1968: Atmospheric water vapor transport and the water balance cf North America: Part II, Large-scale water balance investigations. Mon. Wea. Rev., 96, pp. 720-734.

Rowntree, P. R. and J. A. Bolton, 1978: Experiments with soil moisture anomalies over Europe. The GARP Programme on Numerical Experimentation: Research Activities in Atmospheric and Ocean Modelling, (Ed. R. Asselin). Report No. 18. WMO/ICSU, Geneva, August 1978, p. 63.

Rutter, A. J., 1975: The hydrological cycle in vegetation. In Vegetation and the Atmosphere, Vol. II, Case Studies. (Ed. J. L. Monteith). Academic Press, New York/London. pp. 111-154.

Suarez, M. J., A. Arakawa and D. A. Randall: The parameterization of the planetary boundary layer in the UCLA general circulaton model: formulation and results. Mon. Wea. Rev. (in press)

Schutz, C. and W. L. Gates, 1972: Global Climatic Data for Surface, 800 mb, 400 mb: July. Rand Report. R-915-ARPA, The Rand Corporation, Santa Monica, Calif. pp.

Sellers, P. and J. G. Lockwood, 1981: A Numerical Simulation of the Effects of Changing Vegetation Type on Surface Hydroclimatology. Climatic Change, 3, pp. 121-136.

Shukla, J. and Y. Mintz, 1981: Influence of land-surface evapotranspiration on the earth's climate. (Presented at the JSC Study Conference on Land-Surface Processes in Atmospheric General Circulation Models, Greenbelt, U.S.A., 5-10 January 1981). Published in Science, 215, pp. 1498-1501, 1982.

Shukla, J., D. Randall, D. Straus, Y. Sud and L. Marx, 1981: Winter and Summer Simulations with the GLAS Climate Model. NASA Technical Memorandum 83866, Goddard Space Flight Center, Greenbelt, Md.   282 pp.

Shuttleworth, W. J. and I. R. Calder, 1979: Has the Priestley-Taylor Equation Any Relevance to Forest Evaporation? J. Appl. Meteor., 18, pp. 639-646.

Somerville, R. C. J., P. H. Stone, M. Halem, J. E. Hansen, J. S. Hogan, L. M. Druyan, G. Russell, A. A. Lacis, W. J. Quirk and J. Tenenbaum, 1974: The GISS model of the global atmosphere. J. Atmos. Sci., 31, pp. 84-117.

Stone, P. H., S. Chow and W. J. Quirk, 1977: July climate and a comparison of the January and July climates simulated by the GISS general circulation model. Mon. Wea. Rev., 105, pp. 170-194.

Walker, J. M. and Rowntree, P. R., 1977: The effect of soil moisture on circulation and rainfall in a tropical model. Quart. J. R. Met. Soc., 103, pp. 29-46.

Washington, W. M. and D. L. Williamson, 1977: A description of the NCAR global circulation models. Methods in Computational Physics, 17, pp. 111-172.

WMO, 1979: Report of the JOC Study Conference on Climate Models: Performance, Intercomparison and Sensitivity Studies. Washington, D. C., 3-7 April 1978. (ed. L. Gates) GARP Publication Series No. 22. WMO, Geneva.

ORIGINAL PAGE IS
OF POOR QUALITY